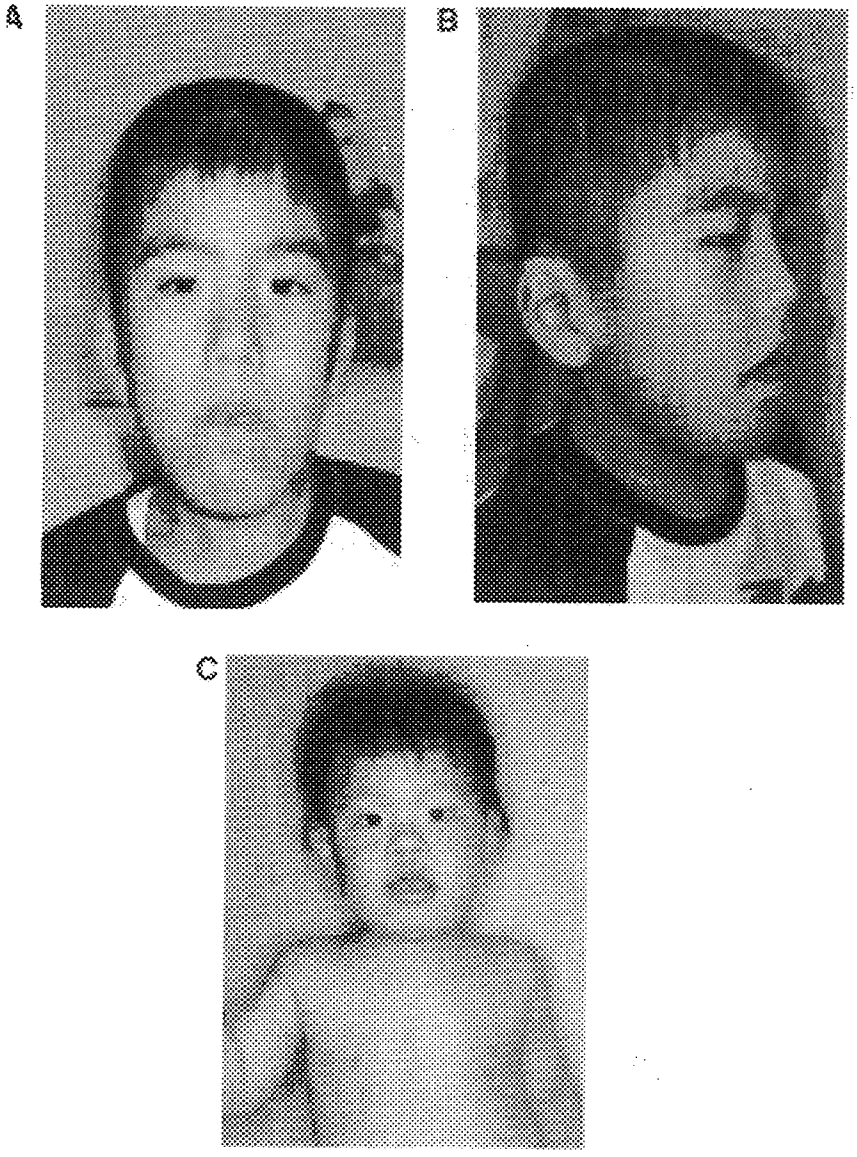

FIG. 1. Patient 4 at age 7 years (**A** and **B**) and Patient 7 at age 18 months (**C**). Note a tongue groove (A and B) and accessory nipples (C). [Color figure can be viewed in the online issue, which is available at www.interscience.wiley.com.]

short 273-bp products both in the patient and his mother (Fig. 2A). Direct sequencing of the 273-bp fragment indicated a deletion of 35,074-bp (between g.132445395 and g.132480524) spanning introns 6 and 7 and including entire exon 7 (Fig. 2B).

DISCUSSION

All seven patients we studied had typical clinical manifestations of SGBS, including pre- and postnatal overgrowth, and a characteristic face that became "coarse" during childhood (Table I). All seven patients were found to have a mutation in *GPC3*; one patient had a large deletion, four had single-base substitutions, one had a single-base insertion, and the other had a combination of a six-base deletion and a three-base insertion—all resulting in loss-of-function of glypican-3. These deletions/mutations were detected in exons 2, 3, 4, and 7 of *GPC3*.

A deletion study by Pilia et al. [1996] examined six of the eight exons of *GPC3* in six families with SGBS, and identified deletions in three families. One (family a) of the three families, later turned out to have a 13-bp deletion and a consequent frameshift in exon 2 [Xuan et al., 1999]. This suggested that large deletions might be responsible for a significant proportion of cases of SGBS. This would not be unreasonable given the large region of genomic DNA covered by *GPC3*. Subsequent deletion studies, including those that analyzed all eight exons of *GPC3*, detected 13 families and sporadic patients with deletions among 43 families and patients studied, giving a frequency of 30% [Hughes-Benzie et al., 1996; Lindsay et al., 1997; Veugelers et al., 1998; Li et al., 2001]. These

TABLE II. Primers Used for PCR and Sequencing

PCR primer		Product length (base pairs)	Intron in amplicon (base pairs)
GPC3exon1F	CAGGTAGCTGCGAGGAAACT		
GPC3exon1R	ctcagggtacagccaccac	393	53
GPC3exon2F	ggtgtgggtgtgtgagagag		40
GPC3exon2R	gcccaaataatgatgccact	277	21
GPC3exon3F	ttttcacactggattttcatgc		47
GPC3exon3R	tacctgctactggccacctc	831	47
GPC3exon4F	tgggggaagaaattgaagtg		70
GPC3exon4R	tttcactctagtggtttttgacctt	302	52
GPC3exon5F	ttgcctcttatgcacagatgtt		15
GPC3exon5R	tttctggtgcaattaatggaga	267	82
GPC3exon6F	gcttttcctttgtttgggact		38
GPC3exon6R	ctctctctctcccccctcctc	255	55
GPC3exon7F	tgcagacccacctgagaaat		37
GPC3exon7R	ttgtgtgttgcagggaatgt	327	90
GPC3exon8F	gctcgagctgtgcatagtgt		72
GPC3exon8R	CCCTTTATCGAGGAAGACCAC	306	
Reading primer in exon 3			
GPC3exon3internalFor	GAGCAAGACGTGACCTGAAA		
GPC3exon3internalRev	CGGCCACAGTCCTTACTGA		
Intronic primers placed introns 6 and 7			
Intronic primer6	ccacatggcttctgtccagag		
Intronic primer7	cccagtgcttcttcttgtgcta		

Capital letter sequences are quoted from cDNA and lower-case letter sequences from genomic introns.

studies involved PCR amplification of the exons of *GPC3* of genomic DNA. The gene is not expressed in readily available samples such as blood cells or fibroblasts, so that its cDNA is not easily accessible. The deletions detected in these studies ranged in size from one to six exons, covered all eight exons of *GPC3*, and in some instances involved exon 8 and extended to the centromere [Hughes-Benzie et al., 1996; Lindsay et al., 1997; Veugelers et al., 1998].

Mutation status of *GPC3* was analyzed in five studies, and three large deletions and nine mutations were identified among 15 families and sporadic patients with SGBS [Okamoto et al., 1999; Xuan et al., 1999; Veugelers et al., 2000; Mariani et al., 2003; Rodriguez-Criado et al., 2005]. The frequency of large-scale deletions (20%) was much less than previously thought. Other mutations encountered included nonsense mutations (three cases), a missense mutation (one case), frameshift mutations (three cases), and splice-site mutations (two cases). These studies may be biased toward the patients with typical clinical manifestations of the syndrome, although no correlation has been noted between the location and nature of mutations and the phenotype of the patients studied. Possible exceptions to the rule are males in family SGB-5 reported by Lindsay et al. [1997] with deletion of exons 4 and 5, and a patient by Li et al. [2001] with a deletion of exon 8. These patients had atypical facies.

In conclusion, we identified a gross deletion and loss-of-function mutations in all seven patients with typical SGBS studied. Further mutation studies are desirable of patients with both typical and atypical clinical manifestations of SGBS.

ACKNOWLEDGMENTS

We thank patients and their families for their participation in this study. This work was supported in part by a grant for Research on Children and Families from the Ministry of Health, Labor, and Welfare of Japan, and Kawano Masanori Memorial Foundation for Promotion of Pediatrics.

TABLE III. *GPC3* Mutations Detected in Seven Patients with SGBS

Patient	Exon	Mutation[a]	Type of mutation	Amino acid change[b]
1	3	c. 760C > T	Nonsense	p. Arg254X
2	3	c. 691C > T	Nonsense	p. Gln231X
3	4	c. 1159C > T	Nonsense	p. Arg387X
4.	2	c. 240dupA	Frameshift	p. Tyr81IlefsX36
5	3	c. 780_785del insAGC	Nonsense	p. Trp260X
6	2	c. 256 C > T	Nonsense	p. Arg86X
7	7	g. 132445395–132480524 del	Deletion	

Data are from the coding sequence of *GPC3* (NM_004484), and data for Patient 7 are from the genomic sequence database (Ensembl v34).
[a]Experimentally determined.
[b]Theoretically deduced.

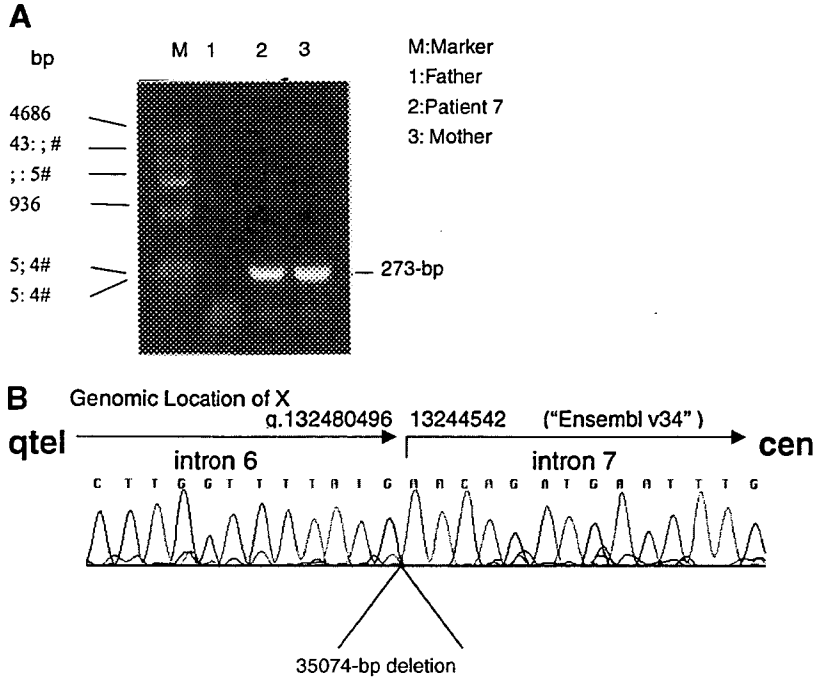

FIG. 2. *GPC3* mutation identified in Patient 7. **A**: Abnormally short PCR products of 273 bp are seen in both Patient 7 and his mother, when using a primer set spanning introns 6 and 7. **Lanes M, 1, 2,** and **3** are a size marker, father, Patient 7, and mother, respectively. **B**: Electropherogram of direct sequence of the patient's PCR product indicating a 35,074-bp deletion between introns 6 and 7. Deletion extent was based on the genomic sequence database, Ensembl v34.

REFERENCES

Huber R, Crisponi L, Mazzarella R, Chen CN, Su Y, Shizuya H, Chen EY, Cao A, Pilia G. 1997. Analysis of exon/intron structure and 400 kb of genomic sequence surrounding the 5′-promoter and 3′-terminal ends of the human glypican 3 (GPC3) gene. Genomics 45:48–58.

Hughes-Benzie RM, Pilia G, Xuan JY, Hunter AG, Chen E, Golabi M, Hurst JA, Kobori J, Marymee K, Pagon RA, Punnett HH, Schelley S, Tolmie JL, Wohlferd MM, Grossman T, Schlessinger D, MacKenzie AE. 1996. Simpson–Golabi–Behmel syndrome: Genotype/phenotype analysis of 18 affected males from 7 unrelated families. Am J Med Genet 66:227–234.

Lapunzina P. 2005. Risk of tumorigenesis in overgrowth syndromes: A comprehensive review. Am J Med Genet Part C 137C:53–71.

Li M, Shuman C, Fei YL, Cutiongco E, Bender HA, Stevens C, Wilkins-Haug L, Day-Salvatore D, Yong SL, Geraghty MT, Squire J, Weksberg R. 2001. GPC3 mutation analysis in a spectrum of patients with overgrowth expands the phenotype of Simpson–Golabi–Behmel syndrome. Am J Med Genet 102:161–168.

Lindsay S, Ireland M, O'Brien O, Clayton-Smith J, Hurst JA, Mann J, Cole T, Sampson J, Slaney S, Schlessinger D, Burn J, Pilia G. 1997. Large scale deletions in the GPC3 gene may account for a minority of cases of Simpson–Golabi–Behmel syndrome. J Med Genet 34:480–483.

Mariani S, Iughetti L, Bertorelli R, Coviello D, Pellegrini M, Forabosco A, Bernasconi S. 2003. Genotype/phenotype correlations of males affected by Simpson–Golabi–Behmel syndrome with GPC3 gene mutations: Patient report and review of the literature. J Pediatr Endocrinol Metab 16:225–232.

Neri G, Marini R, Cappa M, Borrelli P, Opitz JM. 1988. Simpson–Golabi–Behmel syndrome: An X-linked encephalo–trophoschisis syndrome. Am J Med Genet 30:287–299.

Okamoto N, Yagi M, Imura K, Wada Y. 1999. A clinical and molecular study of a patient with Simpson-Golabi–Behmel syndrome. J Hum Genet 44:327–329.

Pellegrini M, Pilia G, Pantano S, Lucchini F, Uda M, Fumi M, Cao A, Schlessinger D, Forabosco A. 1998. Gpc3 expression correlates with the phenotype of the Simpson–Golabi–Behmel syndrome. Dev Dyn 213:431–439.

Pilia G, Hughes-Benzie RM, MacKenzie A, Baybayan P, Chen EY, Huber R, Neri G, Cao A, Forabosco A, Schlessinger D. 1996. Mutations in GPC3, a glypican gene, cause the Simpson–Golabi–Behmel overgrowth syndrome. Nat Genet 12:241–247.

Rodriguez-Criado G, Magano L, Segovia M, Gurrieri F, Neri G, Gonzalez-Meneses A, Gomez de Terreros I, Valdez R, Gracia R, Lapunzina P. 2005. Clinical and molecular studies on two further families with Simpson–Golabi–Behmel syndrome. Am J Med Genet Part A 138A:272–277.

Sambrook J, Russell DW. 2001. Touch down PCR. In: Sambrook J, Russell DW, editors. Molecular Cloning. Cold Spring Harbor, New York: Cold Spring Harbor Laboratory Press. p 112.

Terespolsky D, Farrell SA, Siegel-Bartelt J, Weksberg R. 1995. Infantile lethal variant of Simpson–Golabi–Behmel syndrome associated with hydrops fetalis. Am J Med Genet 59: 329–333.

Veugelers M, Vermeesch J, Watanabe K, Yamaguchi Y, Marynen P, David G. 1998. GPC4, the gene for human K-glypican, flanks GPC3 on xq26: Deletion of the GPC3-GPC4 gene cluster in one family with Simpson–Golabi–Behmel syndrome. Genomics 53:1–11.

Veugelers M, Cat BD, Muyldermans SY, Reekmans G, Delande N, Frints S, Legius E, Fryns JP, Schrander-Stumpel C, Weidle B, Magdalena N, David G. 2000. Mutational analysis of the GPC3/GPC4 glypican gene cluster on Xq26 in patients with Simpson–Golabi–Behmel syndrome: Identification of loss-of-function mutations in the GPC3 gene. Hum Mol Genet 9:1321–1328.

Xuan JY, Hughes-Benzie RM, MacKenzie AE. 1999. A small interstitial deletion in the GPC3 gene causes Simpson–Golabi–Behmel syndrome in a Dutch–Canadian family. J Med Genet 36:57–58.

0021-972X/07/$15.00/0
Printed in U.S.A.

The Journal of Clinical Endocrinology & Metabolism 92(10):4009–4014

doi: 10.1210/jc.2007-1101

Intact Kinase Homology Domain of Natriuretic Peptide Receptor-B Is Essential for Skeletal Development

Rumi Hachiya, Yuko Ohashi, Yasutomi Kamei, Takayoshi Suganami, Hiroshi Mochizuki, Norimasa Mitsui, Masaaki Saitoh, Masako Sakuragi, Gen Nishimura, Hirofumi Ohashi, Tomonobu Hasegawa, and Yoshihiro Ogawa

Department of Pediatrics (R.H., T.H.), Keio University School of Medicine, 160-8582 Tokyo, Japan; Department of Molecular Medicine and Metabolism, Medical Research Institute (R.H., Y.K., T.S., Y.Og.), and Center of Excellence Program for Frontier Research on Molecular Destruction and Reconstitution of Tooth and Bone (Y.Og.), Tokyo Medical and Dental University, 101-0062 Tokyo, Japan; Divisions of Medical Genetics (Y.Oh., H.O.) and Metabolism and Endocrinology (H.M.), and Department of Clinical Laboratory (N.M.), Saitama Children's Medical Center, 339-8551 Saitama, Japan; Department of Surgery (M.Sai., M.Sak.), Saitama Cardiovascular and Respiratory Center, 360-0105 Saitama, Japan; and Department of Radiology (G.N.), Tokyo Metropolitan Kiyose Children's Hospital, 204-8567 Tokyo, Japan

Context: Natriuretic peptide receptor-B (NPR-B, GC-B in rodents; gene name *NPR2*) is a guanylyl cyclase-coupled receptor that mediates the effect of C-type natriuretic peptide. Homozygous mutations in human NPR-B cause acromesomelic dysplasia, type Maroteaux (OMIM 602875), an autosomal recessive skeletal dysplasia. NPR-B has an intracellular kinase homology domain (KHD), which has no kinase activity, and its functional significance *in vivo* is currently unknown.

Objective: We examined the functional significance of a novel NPR-B KHD mutation in humans.

Patients and Methods: A 28-yr-old Japanese male presented with marked short stature (118.5 cm, −9.3 SD). His limbs showed marked shortening in the middle and distal segments. His parents had relatively short stature with height z-scores of −2.75 and −0.98 (his father and mother, respectively). Direct sequencing of coding region of the *NPR2* gene of the family was performed. The mutant receptor activity was investigated by saturation binding assay and cGMP measurement. Additionally, interaction between the mutant and wild type allele was investigated by the titration experiments.

Results: We identified a novel missense mutation L658F in KHD of NPR-B in homozygous and heterozygous states in the patient and his parents, respectively. The mutation conferred normal binding affinity for C-type natriuretic peptide but no discernible ligand-induced cGMP production. Furthermore, L658F mutant impaired wild-type NPR-B-mediated cGMP production in a dose-dependent manner, suggesting that short stature found in L658F heterozygote can be caused by its dominant-negative effect.

Conclusions: This study provides the first evidence that intact KHD of NPR-B is essential for skeletal development. (***J Clin Endocrinol Metab* 92: 4009–4014, 2007**)

NATRIURETIC PEPTIDE RECEPTOR (NPR)-B [guanylyl cyclase (GC)-B, GC-B in rodents; gene name *NPR2*] is a receptor for C-type natriuretic peptide (CNP) that acts locally as a paracrine and/or autocrine regulator in a wide variety of tissues (1). Using the rodent models, we and others have demonstrated that the CNP/NPR-B pathway plays an important role in the regulation of bone formation *in vivo* (2–11). Recently Bartels *et al.* (12) reported that homozygous mutations in human NPR-B cause acromesomelic dysplasia, type Maroteaux (AMDM; OMIM 602875), a rare autosomal recessive skeletal dysplasia, indicating that NPR-B is also involved in human skeletal growth. This contrasts sharply with the role of NPR-A (GC-A; *NPR1*) that mediates two cardiac natriuretic peptides (atrial natriuretic peptide and brain natriuretic peptide); it is involved in the regulation of cardiovascular homeostasis (13).

Both NPRs (NPR-A and NPR-B) consist of an extracellular ligand binding domain, a single hydrophobic transmembrane region, an intracellular kinase homology domain (KHD), and carboxyl-terminal GC domain (1, 13). The KHD of NPRs is highly conserved in structure among species and is unique in that it has no kinase activity. However, the physiological role of KHD *in vivo* is poorly understood.

Here we report a novel homozygous missense mutation in KHD of NPR-B (L658F) in a Japanese patient with AMDM. Using the *in vitro* functional assay, we demonstrated that the mutation confers normal ligand binding affinity but impaired ligand-induced GC activity. This study represents the first demonstration that KHD of NPR-B is essential for bone development *in vivo*.

Patients and Methods

This study was conducted with informed consent from the patient and his parents and approved by the institutional review boards at Keio University School of Medicine, Saitama Children's Medical Center, and Medical Research Institute, Tokyo Medical and Dental University.

First Published Online July 24, 2007

Abbreviations: AMDM, Acromesomelic dysplasia, type Maroteaux; Bmax, maximum binding; CNP, C-type natriuretic peptide; GC, guanylyl cyclase; HA, hemagglutinin; Kd, dissociation constant; KHD, kinase homology domain; NPR, natriuretic peptide receptor; WT, wild type.

Case report

The patient is the second child of Japanese parents who are first cousins. He was born after vacuum extraction due to a nuchal cord at 40 wk of gestation. His birth weight was 3600 g (+0.92 SD), length 51 cm (+0.53 SD), and occipital-frontal circumference was 36 cm (+1.7 SD). He was initially given a diagnosis of achondroplasia at 3 months of age because of the short limb and relative macrocephaly. At the age of 28 yr, he was referred to Saitama Children's Medical Center for further examination. At the initial visit, his height was 118.5 cm (−9.3 SD), his weight was 34.5 kg (−2.7 SD), and his head circumference was 57.1 cm (+0.92 SD). He had a long face, hypertelorism, and a slightly flattened midface. His fingers were extremely short and broad, his first toes were relatively large, and the skin of his fingers was redundant. His limbs showed marked shortening in the middle and distal segments (Fig. 1, A–C). A skeletal survey revealed disproportionate mesomelic shortening of the arms with bowing of the radius, shortening of the phalanges and metacarpal bones, and mild platyspondyly and mild interpediculate narrowing of the vertebral column (Fig. 1, D and E). His intelligence was normal. Based on these observations, we concluded that he has AMDM rather than achondroplasia. He had been well except for the marked short stature until the age of 27 yr, when he was diagnosed as having abdominal aortic pseudoaneurysm by computed tomography scanning and was surgically treated with a stent graft. Six months after the operation, he had recurrence of pseudoaneurysm on the right common iliac artery (Fig. 1F) and underwent covered stent. There were no other AMDM patients in his family (Fig. 2A). His father was 155 cm (−2.75 SD) and his mother was 153 cm (−0.98 SD) in height. His elder brother was stillborn due to a nuchal cord. His elder sister was healthy.

Mutation analysis

We screened the patient and his parents for *NPR2* mutations. Genomic DNA was extracted from their peripheral blood using standard techniques. Bidirectional direct sequencing of *NPR2* using BigDye terminator cycle sequencing kit (version 1.1; Applied Biosystems, Foster City, CA) was analyzed with ABI 3130x automated sequencer (Applied Biosystems). The primers were designed to amplify all exons and exon-intron boundaries according to the published *NPR2* genomic DNA sequences (Ensembl Genome Browser accession no. ENSG00000159899). The primer sequences and PCR conditions are available upon request.

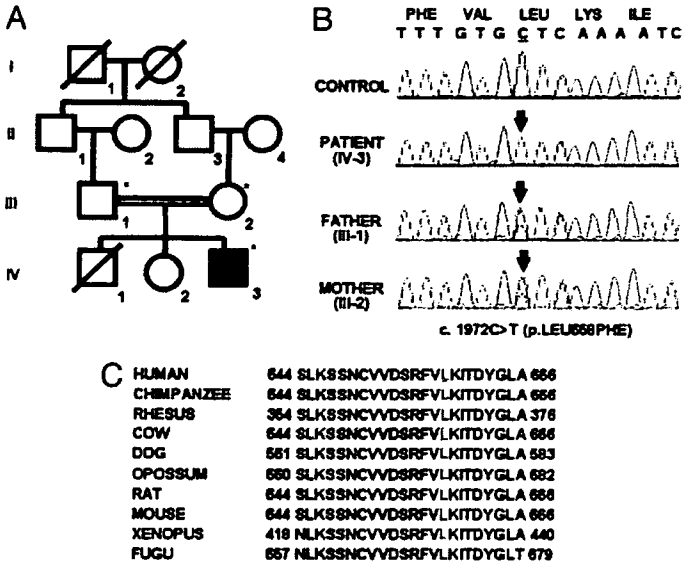

FIG. 2. Identification of *NPR2* mutation. A, Pedigree of the family of patient IV-3. *, Examined personally. B, Homozygous and heterozygous missense mutations (c.1972C>T) were detected in *NPR2* in the patient and his parents, respectively. c., cDNA, p., protein. C, Amino acid alignment of NPR-B among species. Leucine at codon 658 is in the highly conserved region (*highlighted*) in KHD.

Expression constructs and site-directed mutagenesis

The full-length cDNA clone of human NPR-B (GenBank accession no. BC096343; American Type Culture Collection, Manassas, VA) was subjected to PCR using adapter primers to introduce *Hin*dIII and *Xho*I sites into 5′ of the start codon and 3′ of the stop codon, respectively. The 3.1-kb insert was isolated from PCR product by *Hin*dIII and *Xho*I digestion and ligated into the pcDNA3.1 expression vector to generate pcDNA3.1/NPR-B wild-type (WT). To generate expression vectors with the hemagglutinin (HA) epitope immediately 3′ of the expected cleavage site of

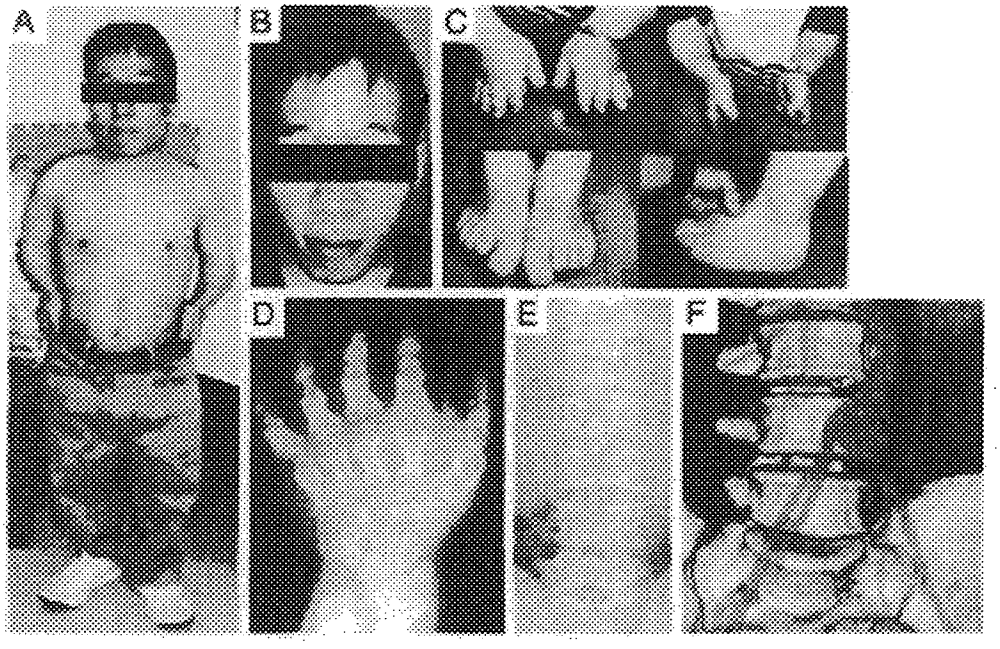

FIG. 1. Clinical features of the patient. A, Front full-length portrait. B, Face photograph. C, Hands and feet photographs. D, Hand radiograph. E, Spine radiograph. Note mild platyspondyly and interpediculate narrowing as revealed by the reduction in the L1-L5 heights and interpediculate distance, respectively. F, Three-dimensional computed tomography angiography revealed the pseudoaneurysm on right common iliac artery.

the signal sequence (~nucleotide +66), *Sac*II and *Hpa*I sites were created by site-directed mutagenesis at nucleotides +55 to +60 and +67 to +72, respectively. Linkers encoding the HA epitope were inserted between the *Sac*II and *Hpa*I sites to generate the HA-tagged wild-type clone; pcDNA3.1/HA-NPR-B wild-type (HA-WT). The mutant clone c.1972C>T (p.L658F) was generated by site-directed mutagenesis (QuikChange site-directed mutagenesis kit; Stratagene, La Jolla, CA) from WT and HA-WT as pcDNA3.1/NPR-B L658F (L658F) and pcDNA3.1/HA-NPR-B L658F (HA-L658F), respectively (Fig. 3A). All the expression vector constructs were verified by DNA sequencing.

Cell culture and transfection

COS-7 cells were seeded to 0.5–1 × 10^5 cells/cm^2 in 12- or 24-well plates in DMEM with 10% fetal bovine serum. The cells were transfected with pcDNA3.1 (mock), HA-WT, and HA-L658F alone or a combination of HA-WT and L658F in the titration experiments with Lipofectamine 2000 (Invitrogen, Carlsbad, CA). In the titration experiments, COS-7 cells were cotransfected with differing ratios of HA-WT and L658F DNAs with the amount of HA-WT DNA constant. The total amount of DNAs transfected was kept constant using the mock. The cells were used for the experiment 48 h after transfection.

Immunoblotting analysis

The transfected cells in 12-well plates were scraped into 150 μl/well of the lysis buffer [20 mM Tris (pH 7.4), 5 mM EDTA, 10 mM $Na_4P_2O_7$, 100 mM NaF, 1% Nonidet-P, 10 μg/ml aprotinin, 10 μg/ml leupeptin, 1 mM phenylmethylsulfonyl fluoride, 2 mM Na_3VO_4], sonicated for 1 sec, and centrifuged at 17,000 × *g* for 15 min. The supernatant was fractionated on a 7.5% sodium dodecyl sulfate-polyacrylamide gel and blotted to the polyvinylidene defluoride transfer membrane (PerkinElmer, Waltham, MA). The HA-tagged NPR-B was detected by HA-tag (6E2) mouse monoclonal antibody (1:1000; Cell Signaling Tech-

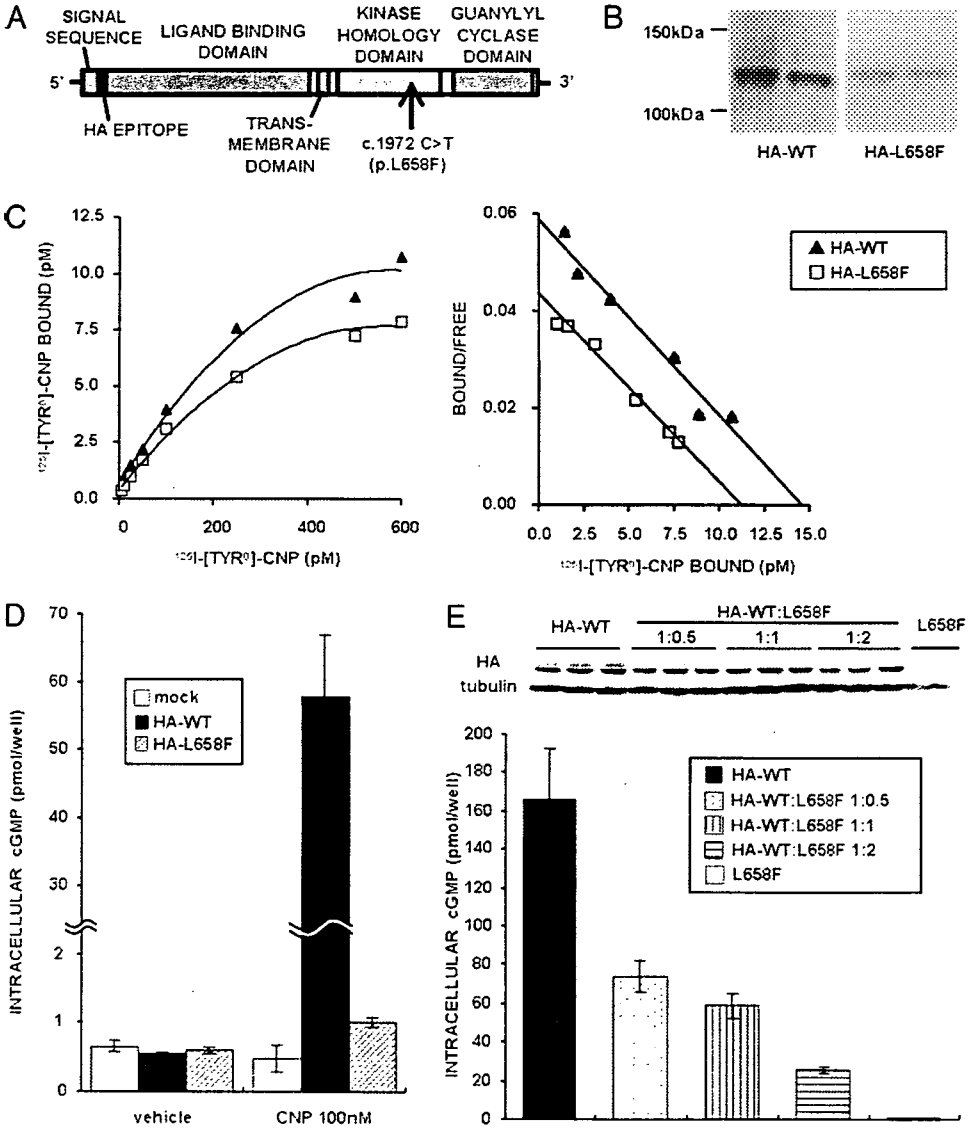

FIG. 3. *In vitro* functional assay. A, Schematic representation of *NPR2* cDNA with the HA epitope. The *upward arrow* denotes the nucleotide mutated by site-directed mutagenesis. B, NPR-B protein expression in COS-7 cells transfected with HA-WT or HA-L658F. Representative Western blots with anti-HA antibody are shown. C, CNP binding to NPR-B. *Left panel*, Binding of ^{125}I-[Tyr^0]-CNP to COS-7 cells expressing HA-WT or HA-L658F examined by saturation binding analysis. *Right panel*, Scatchard analysis. Linear regression curves are shown by *solid lines*. D, cGMP measurement. E, Dose-dependent effect of L658F on HA-WT. The ratios of HA-WT and L658F are those of transfected DNA concentrations. COS-7 cells were transfected with the constant amount of HA-WT. The total amount of DNAs transfected was kept constant in all transfections using mock. *Upper panel*, Representative Western blots with anti-HA and antitubulin are shown. Note HA-WT protein levels are roughly constant irrespective of the DNA concentrations of L658F mutant. *Lower panel*, cGMP production.

nology, Beverly, MA) using ECL plus detection system (GE Healthcare Bio-Science, Piscataway, NJ) with ECL antimouse IgG, horseradish peroxidase-linked sheep antibody (1:1000; GE Healthcare Bio-Science). As an internal control for the titration experiments, α-tubulin was detected by monoclonal anti-α-tubulin antibody (1:4000; Sigma-Aldrich, St. Louis, MO) and antimouse IgG antibody (1:10,000).

Saturation binding assay

Saturation binding assay with the intact cells were carried out as described with slight modification (14, 15). The transfected intact cells in 24-well plates were washed once with 200 μl of DMEM containing 0.1% BSA. Cells were then incubated at 37 C for 1 h with same medium with ^{125}I-[Tyr^{0}]-CNP (Peninsula Laboratories, San Carlos, CA) at various concentrations with or without 0.5 μM nonradioactive CNP (Bachem, Bubendorf, Switzerland) to define nonspecific binding. The cells were washed four times with 200 μl PBS containing 0.1% BSA and solubilized with 1 ml 0.5 N NaOH. Radioactivity of the cell lysate was counted.

cGMP assay

The transfected cells were serum starved for 12 h before cGMP assay and then incubated at 37 C in DMEM containing 0.1% BSA and 0.5 mM 3-isobutyl-1-methylxanthine, a phosphodiesterase inhibitor, for 10 min. The cells were treated with CNP (100 nM) or vehicle (PBS containing 0.1% BSA) and incubated for another 10 min. The stimulations were stopped with 0.1 M HCl, and cGMP was measured by the competitive enzyme immunoassay according to the supplier's instruction manual (cGMP enzyme immunoassay kit; Cayman Chemical, Ann Arbor, MI).

Statistics

Data were expressed as the mean ± SE. Dissociation constant (Kd) was determined using the inverse of the slope of the linear regression curves obtained by the Scatchard plot. Maximum binding (Bmax) was determined by extrapolation of the linear regression curves to the abscissa.

Results

Identification of NPR2 mutation

We identified a novel C>T missense mutation at the nucleotide position +1972 (c.1972C>T) that creates a leucine>phenylalanine substitution (p.L658F) in homozygous and heterozygous states in the patient and his parents, respectively (Fig. 2B). This variant was not reported as a single nucleotide polymorphism in dbSNP (http://www.ncbi.nlm.nih.gov/projects/SNP/) and JSNP (http://snp.ims.u-tokyo.ac.jp/) databases and not found in 100 alleles from Japanese healthy controls (data not shown). L658 is located in the highly conserved region in KHD of NPR-B or GC-B among species (Fig. 2C).

In vitro functional assay

To investigate the functional significance of the L658F mutation, we performed *in vitro* functional assay. COS-7 cells were transfected with HA-WT and mutant (HA-L658F) constructs, and the whole-cell extracts were resolved by SDS-PAGE and Western blotting. Western blot analysis confirmed that both HA-WT and HA-L658F are expressed in COS-7 cells with an approximate molecular size of 120 kDa (Fig. 3B).

In saturation binding assay, HA-WT and HA-L658F were capable of binding CNP with similar affinity (Fig. 3C, *left panel*). Scatchard plot analysis revealed a single class of high-affinity CNP binding sites for HA-WT and HA-L658F (HA-WT: Bmax 14.5 pM, Kd 246 pM; HA-L658F: Bmax 11.4 pM, Kd 266 pM) (Fig. 3C, *right panel*).

We also examined cGMP production in the cells transfected with HA-WT or HA-L658F. Treatment with CNP at a dose of 100 nM increased intracellular cGMP levels by more than 100-fold in HA-WT-transfected cells relative to mock-transfected cells (Fig. 3D). However, there was no significant difference between mock- and HA-L658F-transfected cells, when treated with CNP.

Dose-dependent effect of L658F on HA-WT cGMP production and expression was analyzed by the titration experiments. With HA-WT protein levels being roughly constant irrespective of the amount of the mutant, intracellular cGMP accumulation on CNP stimulation at a dose of 100 nM was abolished with increasing amounts of L658F (Fig. 3E).

Discussion

Here we identified a novel homozygous missense mutation in KHD of NPR-B in a Japanese patient with AMDM. We demonstrated that intact KHD of NPR-B is essential for skeletal development *in vivo*. The physiological role of KHD *in vivo* has been poorly understood so far; there have been no reports on animal models carrying KHD mutations. Moreover, the two missense mutations of KHD of NPR-B (Y708C and R776W) found in patients with AMDM were not functionally investigated (12). This study provides evidence that L658F, a missense mutation of KHD, markedly impairs ligand-induced cGMP production in a patient with AMDM. These observations indicate that KHD of NPR-B is essential for skeletal development *in vivo*.

It is likely that KHD is important for GC activation upon ligand binding. In this study, we found that L658F mutant binds CNP with normal affinity but does not lead to enzyme activation. Chinkers and Garbers (16) provided *in vitro* evidence that complete deletion of KHD from NPR-A results in constitutive activation of GC in the absence of the ligand and suggested that KHD of NPRs represses the enzymatic activity without ligand stimulation, which, upon ligand binding, is released and activated. *In vitro* studies with partial deletion or mutagenesis of KHD showed that putative ATP binding motif (^{519}LXGXXXG^{525}) and phosphorylation sites (S513, T516, S518, S523, S526) are important for the receptor activation (17, 18). In this regard, Potter *et al.* (19) proposed a model for signal transduction; ATP binding and phosphorylation in KHD is required for sensitization of NPRs, which is followed by ligand-induced conformational change and enzyme activation. Because L658F mutant may not affect ATP binding and phosphorylation, we speculate that upon ligand binding, L658F mutant does not take properly the ligand-induced conformational change for enzyme activation. Further studies are required to elucidate the functional role of KHD in NPR-B signal transduction.

It is conceivable that NPR-B is involved in the regulation of endochondral ossification in humans. The patient described herein had marked shortening of the long bones and vertebrae, but his head circumference was within the normal range, suggesting the impairment of endochondral ossification. The precise role of NPR-B in human endochondral

ossification is currently unknown because growth plate histology has not been available from the patients with AMDM. The vertebrate models, mostly rodent models, have been useful to understand the human skeletal biology (20). Lacking CNP or GC-B, for instance, results in impaired endochondral ossification and severe dwarfism in mice (2, 3), and a natural mutation in the GC domain of GC-B in mice causes dwarfism (4), whereas transgenic overexpression (5–7) or reduced clearance (8, 9) of the ligands causes skeletal overgrowth. Moreover, targeted deletion or natural mutation of cGMP-dependent protein kinase II, a downstream target of cGMP, leads to the impairment of endochondral ossification (10, 11). Importantly, overexpression of CNP in chondrocytes has rescued a mouse model of achondroplasia (7). The above observations with rodents support the concept that NPR-B is involved in the regulation of human endochondral ossification.

The data of this study also suggest that short stature found in his parents is caused by a dominant-negative effect of the mutant allele. They are heterozygous for L658F mutation and have relatively short stature with height z-scores of −2.75 and −0.98 (for his father and mother, respectively). This study demonstrates that L658F mutant impairs the wild-type NPR-B-mediated cGMP production in a dose-dependent manner. Because L658F mutant has the intact extracellular domain required for dimerization (21), it is likely that L658F mutant forms a heterodimer with the wild-type NPR-B, thereby interfering its signal transduction in a dominant-negative fashion. In this regard, two recent studies (12, 22) reported that heterozygous carriers of NPR-B are associated with short stature, and the authors discussed that the haploinsufficiency may be the cause. On the other hand, Tamura and colleagues (3, 17) demonstrated that an alternatively spliced isoform of murine GC-B named GC-B2, which lacks a 25-amino acid stretch in KHD, acts as a dominant-negative isoform by virtue of blocking homodimer formation of the full-length GC-B1. Furthermore, Langenickel *et al.* (23) reported that a truncated GC-B mutant lacking most of the cytoplasmic domain acts as a dominant-negative molecule *in vitro* and *in vivo*. These observations are also consistent with the hypothesis that the dominant-negative effect can be the cause of short stature in heterozygous carriers of L658F mutation.

The patient had abdominal aortic pseudoaneurysm at the age of 27 yr. Given that NPR-B is expressed in a broad array of tissues including chondrocytes, brain, lung, uterus, and blood vessel (1, 3), it is conceivable that abdominal aortic pseudoaneurysm is related with NPR-B expression in the vessel wall. Further case reports are needed to better characterize the phenotype outside the skeleton, the prognosis and genotype-phenotype correlation of NPR-B mutations.

In conclusion, we report a novel homozygous missense mutation in KHD of NPR-B in a Japanese patient with AMDM. This study provides the first evidence that intact KHD of NPR-B is essential for skeletal development, thereby leading to the better understanding of the molecular mechanisms underlying skeletal development as well as the natriuretic peptide receptor biology.

Acknowledgments

The authors thank the patient and his parents for participation in this study. We also acknowledge Takao Takahashi for fruitful discussion and Shin-ichi Suga for advice on the binding assay.

Received May 17, 2007. Accepted July 18, 2007.

Address all correspondence and requests for reprints to: Yoshihiro Ogawa, Department of Molecular Medicine and Metabolism, Medical Research Institute, Tokyo Medical and Dental University, 2-3-10 Kanda-surugadai, Chiyoda-ku, Tokyo 101-0062, Japan. E-mail: ogawa.mmm@mri.tmd.ac.jp.

This work was supported in part by a Grant-in-Aid for Scientific Research from the Ministry of Education, Culture, Sports, Science, and Technology of Japan; the Ministry of Health, Labor, and Welfare of Japan; the Foundation for Growth Science; and Kawano Masanori Memorial Foundation for Promotion of Pediatrics.

Disclosure Statement: The authors have nothing to declare.

References

1. **Schulz S** 2005 C-type natriuretic peptide and guanylyl cyclase B receptor. Peptides 26:1024–1034
2. **Chusho H, Tamura N, Ogawa Y, Yasoda A, Suda M, Miyazawa T, Nakamura K, Nakao K, Kurihara T, Komatsu Y, Itoh H, Tanaka K, Saito Y, Katsuki M, Nakao K** 2001 Dwarfism and early death in mice lacking C-type natriuretic peptide. Proc Natl Acad Sci USA 98:4016–4021
3. **Tamura N, Doolittle LK, Hammer RE, Shelton JM, Richardson JA, Garbers DL** 2004 Critical roles of the guanylyl cyclase B receptor in endochondral ossification and development of female reproductive organs. Proc Natl Acad Sci USA 101:17300–17305
4. **Tsuji T, Kunieda T** 2005 A loss-of-function mutation in natriuretic peptide receptor 2 (Npr2) gene is responsible for disproportionate dwarfism in cn/cn mouse. J Biol Chem 280:14288–14292
5. **Ogawa Y, Itoh H, Tamura N, Suga S, Yoshimasa T, Uehira M, Matsuda S, Shiono S, Nishimoto H, Nakao K** 1994 Molecular cloning of the complementary DNA and gene that encode mouse brain natriuretic peptide and generation of transgenic mice that overexpress the brain natriuretic peptide gene. J Clin Invest 93:1911–1921
6. **Suda M, Ogawa Y, Tanaka K, Tamura N, Yasoda A, Takigawa T, Uehira M, Nishimoto H, Itoh H, Saito Y, Shiota K, Nakao K** 1998 Skeletal overgrowth in transgenic mice that overexpress brain natriuretic peptide. Proc Natl Acad Sci USA 95:2337–2342
7. **Yasoda A, Komatsu Y, Chusho H, Miyazawa T, Ozasa A, Miura M, Kurihara T, Rogi T, Tanaka S, Suda M, Tamura N, Ogawa Y, Nakao K** 2004 Overexpression of CNP in chondrocytes rescues achondroplasia through a MAPK-dependent pathway. Nat Med 10:80–86
8. **Jaubert J, Jaubert F, Martin N, Washburn LL, Lee BK, Eicher EM, Guenet JL** 1999 Three new allelic mouse mutations that cause skeletal overgrowth involve the natriuretic peptide receptor C gene (Npr3). Proc Natl Acad Sci USA 96:10278–10283
9. **Matsukawa N, Grzesik WJ, Takahashi N, Pandey KN, Pang S, Yamauchi M, Smithies O** 1999 The natriuretic peptide clearance receptor locally modulates the physiological effects of the natriuretic peptide system. Proc Natl Acad Sci USA 96:7403–7408
10. **Pfeifer A, Aszodi A, Seidler U, Ruth P, Hofmann F, Fassler R** 1996 Intestinal secretory defects and dwarfism in mice lacking cGMP-dependent protein kinase II. Science 274:2082–2086
11. **Chikuda H, Kugimiya F, Hoshi K, Ikeda T, Ogasawara T, Shimoaka T, Kawano H, Kamekura S, Tsuchida A, Yokoi N, Nakamura K, Komeda K, Chung UI, Kawaguchi H** 2004 Cyclic GMP-dependent protein kinase II is a molecular switch from proliferation to hypertrophic differentiation of chondrocytes. Genes Dev 18:2418–2429
12. **Bartels CF, Bukulmez H, Padayatti P, Rhee DK, van Ravenswaaij-Arts C, Pauli RM, Mundlos S, Chitayat D, Shih LY, Al-Gazali LI, Kant S, Cole T, Morton J, Cormier-Daire V, Faivre L, Lees M, Kirk J, Mortier GR, Leroy J, Zabel B, Kim CA, Crow Y, Braverman NE, van den Akker F, Warman ML** 2004 Mutations in the transmembrane natriuretic peptide receptor NPR-B impair skeletal growth and cause acromesomelic dysplasia, type Maroteaux. Am J Hum Genet 75:27–34
13. **Garbers DL, Chrisman TD, Wiegn P, Katafuchi T, Albanesi JP, Bielinski V, Barylko B, Redfield MM, Burnett Jr JC** 2006 Membrane guanylyl cyclase receptors: an update. Trends Endocrinol Metab 17:251–258.
14. **Suga S, Nakao K, Hosoda K, Mukoyama M, Ogawa Y, Shirakami G, Arai H, Saito Y, Kambayashi Y, Inouye K, Imura H** 1992 Receptor selectivity of natriuretic peptide family, atrial natriuretic peptide, brain natriuretic peptide, and C-type natriuretic peptide. Endocrinology 130:229–239
15. **Thompson DK, Garbers DL** 1995 Dominant negative mutations of the guanylyl cyclase-A receptor. Extracellular domain deletion and catalytic domain point mutations. J Biol Chem 270:425–430

16. **Chinkers M, Garbers DL** 1989 The protein kinase domain of the ANP receptor is required for signaling. Science 245:1392–1394
17. **Tamura N, Garbers DL** 2003 Regulation of the guanylyl cyclase-B receptor by alternative splicing. J Biol Chem 278:48880–48889
18. **Potter LR, Hunter T** 1998 Identification and characterization of the major phosphorylation sites of the B-type natriuretic peptide receptor. J Biol Chem 273:15533–15539
19. **Potter LR, Abbey-Hosch S, Dickey DM** 2006 Natriuretic peptides, their receptors, and cyclic guanosine monophosphate-dependent signaling functions. Endocr Rev 27:47–72
20. **Karsenty G** 2003 The complexities of skeletal biology. Nature 423:316–318
21. **Chinkers M, Wilson EM** 1992 Ligand-independent oligomerization of natriuretic peptide receptors. Identification of heteromeric receptors and a dominant negative mutant. J Biol Chem 267:18589–18597
22. **Olney RC, Bukulmez H, Bartels CF, Prickett TC, Espiner EA, Potter LR, Warman ML** 2006 Heterozygous mutations in natriuretic peptide receptor-B (NPR2) are associated with short stature. J Clin Endocrinol Metab 91:1229–1232
23. **Langenickel TH, Buttgereit J, Pagel-Langenickel I, Lindner M, Monti J, Beuerlein K, Al-Saadi N, Plehm R, Popova E, Tank J, Dietz R, Willenbrock R, Bader M** 2006 Cardiac hypertrophy in transgenic rats expressing a dominant-negative mutant of the natriuretic peptide receptor B. Proc Natl Acad Sci USA 103:4735–4740

JCEM is published monthly by The Endocrine Society (http://www.endo-society.org), the foremost professional society serving the endocrine community.

International Journal of
HEMATOLOGY

Characterization of Monocyte-Macrophage–Lineage Cells Induced from CD34+ Bone Marrow Cells In Vitro

Kyoko Suzuki,[a,b] Nobutaka Kiyokawa,[a] Tomoko Taguchi,[a] Hisami Takenouchi,[a] Masahiro Saito,[b] Toshiaki Shimizu,[b] Hajime Okita,[a] Junichiro Fujimoto[a]

[a]*Department of Developmental Biology, National Research Institute for Child Health and Development, Tokyo, Japan;* [b]*Department of Pediatrics, Juntendo University, School of Medicine, Tokyo, Japan*

Received November 15, 2006; received in revised form February 13, 2007; accepted February 19, 2007

Abstract

We characterized the expression of cell surface antigens and cytokine-secreting ability of monocyte-macrophage–lineage cells induced in vitro from CD34+ bone marrow cells. After cultivation for 3 weeks, we observed 2 distinct cell fractions: a floating small, round cell fraction and an adherent large, protruding cell fraction. Both cell fractions expressed myelocyte-monocyte–lineage antigens, but mature-macrophage markers such as CD206 were expressed only by the adherent cells. An assessment of cells cultured for 5 weeks revealed spontaneous secretion of interleukin 8 (IL-8) and IL-6, and lipopolysaccharide (LPS)-induced tumor necrosis factor α (TNF-α) secretion in both fractions, but only the adherent cell fraction secreted IL-10 after LPS stimulation. In contrast, both fractions of cells cultured for 3 weeks spontaneously secreted low levels of IL-8, but none of the other cytokines. Upon LPS stimulation, the cells secreted IL-6 and TNF-α, but not IL-10. We also assessed the effect of granulocyte colony-stimulating factor (G-CSF) pretreatment on TNF-α secretion by each cell fraction and found that G-CSF reduced TNF-α secretion only in the adherent fraction of cells cultured for 3 weeks. Monocyte-macrophage–lineage cells induced in vitro should provide an ideal model for functional analysis of monocyte-macrophage cells.
Int J Hematol. 2007;85:384-389. doi: 10.1532/IJH97.06213

Key words: Monocyte-macrophage lineage; Antigen; Cytokine; Expression

1. Introduction

The mononuclear phagocyte system includes a widely distributed family of related cells (such as peripheral blood monocytes, macrophages, Kupffer cells, dendritic cells, osteoclasts, and microglia) that exhibit highly specialized functions. Macrophages resident in a number of tissues act as professional phagocytes and remove pathogens or apoptotic cells [1]. Dendritic cells are specialized to capture and present antigens, initiating the immune response through naive T-cell activation [2]; dendritic cells are also implicated in maintaining tolerance to self antigens [3]. Osteoclasts, multinucleated bone-resorbing cells found in the vicinity of bone, play an essential role in bone remodeling as well as in regulating calcium homeostasis [4]. Microglia represent a unique category of mononuclear phagocytes distributed throughout the central nervous system [5], and in addition to their role as the immune effectors of the central nervous system, they perform nonimmunologic functions, including the production of neurotrophic factors and glutamate uptake [6,7].

The mononuclear phagocytic cells are believed to originate from hematopoietic stem cells in the bone marrow (BM). In the conventional view, monocytes that develop in the BM are released into the circulation and then enter the tissues to become resident macrophages and other mononuclear phagocytic cells [8,9]. Consistent with this view, Kennedy and Abkowitz demonstrated in a mouse transplantation system that more mature monocytes give rise to tissue macrophages, including alveolar macrophages in the lung and Kupffer cells in the liver [10]. The results of a number of studies have suggested, however, that the mechanism of mononuclear phagocytic cell development is more complicated. One intriguing possibility is that less mature marrow-derived cells, such as macrophage colony-forming units, enter

Correspondence and reprints requests: Nobutaka Kiyokawa, MD, PhD, Department of Developmental Biology, National Research Institute for Child Health and Development, 2-10-1, Okura, Setagaya-ku, Tokyo 154-8535, Japan; 81-3-3417-2496; fax: 81-3-3417-2496 (e-mail: nkiyokawa@nch.go.jp).

the tissues and differentiate into macrophages [11]. Prior studies have shown that tissue macrophages divide in situ, indicating that these cells are responsible for the renewal and expansion of this population [12-14].

The functional and phenotypic heterogeneity within the phagocyte system may be evidence of the differentiation plasticity of a common progenitor, but the details of the developmental pathways leading to the maturation of mononuclear phagocytic cells are still unclear. In vitro culture systems in which mature mononuclear phagocytic cells are induced from hematopoietic stem cells or monocyte precursors have been employed in a number of studies to clarify the molecular mechanism of phagocytic cell development. For example, monocyte-macrophage–lineage cells can be induced from CD34⁺ cord blood hematopoietic stem cells by liquid culture with cytokines [15] and by cocultivation with BM stromal cell lines in the presence of cytokines [16]. BM progenitors have recently been identified by their ability to differentiate into dendritic cells or osteoclasts, depending on whether they are exposed to RANKL in combination with granulocyte-macrophage colony-stimulating factor (GM-CSF) or M-CSF [17].

To evaluate the usefulness of monocyte-macrophage–lineage cells as a source for an in vitro model for the functional analysis of a monocytic phagocyte system, we analyzed the immunophenotype of and cytokine production by monocyte-macrophage–lineage cells induced from CD34⁺ BM cells in vitro. In this study, we showed that several distinct developmental stage–related subpopulations are present in monocyte-macrophage–lineage cells induced from CD34⁺ BM cells in vitro.

2. Materials and Methods

2.1. Cells and Reagents

Human BM CD34⁺ cells from Cambrex Bio Science Walkersville (Walkersville, MD, USA) were used. The cells had been isolated from human tissue after informed consent had been obtained. Recombinant human cytokines were purchased from PeproTech (London, UK). Fluorescently conjugated monoclonal antibodies were purchased from Beckman Coulter (Westbrook, MA, USA). Unless otherwise indicated, all other chemical reagents were obtained from Wako Pure Chemical Industries (Osaka, Japan).

2.2. Cultures

Monocyte-macrophage–lineage cells were induced by incubating human BM CD34⁺ cells (1×10^5 cells/well of a 6-well plate) at 37°C under 5% carbon dioxide in 5 mL of 10% (vol/vol) fetal calf serum (Sigma-Aldrich, St. Louis, MO, USA) containing RPMI 1640 medium (Sigma-Aldrich) supplemented with a cytokine mixture consisting of interleukin 3 (IL-3) (20 ng/mL), IL-6 (20 ng/mL), M-CSF (100 ng/mL), GM-CSF (20 ng/mL), and Flt-3 ligand (100 ng/mL) [15,18]. Every week, half of the medium was replaced with fetal calf serum–containing medium supplemented with M-CSF alone. After 3 weeks of cultivation, the medium was completely replaced with the medium supplemented with M-CSF alone, and the cells were cultured for another 2 weeks. At the end of 5 weeks of cultivation, the floating cells in the medium were collected, and the adherent cells were harvested with 0.25% trypsin plus 0.02% EDTA (Immuno-Biological Laboratories Co, Gunma, Japan). These 2 cell fractions were used for further examination.

For the histology studies, cells were harvested and immobilized on glass slides with Cytospin 2 (Shandon, Pittsburgh, PA, USA). After Giemsa staining, cell morphology was assessed by light microscopy (BX-61; Olympus, Tokyo, Japan). Cells were tested for cytokine secretion by exposing the cells to G-CSF and stimulating them with lipopolysaccharide (LPS) (Sigma-Aldrich) for 24 hours, as described previously [19].

2.3. Reverse Transcriptase–Polymerase Chain Reaction Analysis

Total RNA was extracted from cultured human BM cells, and complementary DNA (cDNA) was generated with an RNeasy Mini Kit (Qiagen, Valencia, CA, USA) and a First-Strand cDNA Synthesis Kit (Pfizer, Uppsala, Sweden). cDNA synthesized from 150 ng of total RNA was used as a template for one amplification reaction. The following sets of primers were used: 5′-ttattacccctccttcagacac-3′ (sense) and 5′-aagtctggaaacatctggagagag-3′ (antisense), for amplification of a 347-bp fragment of human tumor necrosis factor α (TNF-α) cDNA; 5′-aagtggtgttctccatgtcc-3′ (sense) and 5′-gagcgaatgacagagggttt-3′ (antisense), for amplification of a 664-bp fragment of human IL-1β cDNA; and 5′-gctggaggactttaagggtt-3′ (sense) and 5′-cccagatccgattttggaga-3′ (antisense), for amplification of a 394-bp fragment of human IL-10 cDNA. The set of primers for amplification of human glyceraldehyde-3-phosphate dehydrogenase was obtained from Stratagene (La Jolla, CA, USA). The polymerase chain reaction (PCR) was repeated for 30 cycles of heating at 94°C for 60 seconds, annealing at 60°C for 30 seconds, and elongation at 72°C for 2 minutes; the PCR products were then separated on a 1.5% agarose gel.

2.4. Immunofluorescence Study and Cytokine Measurement

A multicolor immunofluorescence study was performed with a combination of fluorescein isothiocyanate, phycoerythrin, and phycoerythrin–Cyanine 5 (PC-5). Cells were stained with fluorescently labeled monoclonal antibodies and analyzed by flow cytometry (Epics XL; Beckman Coulter), as described previously [19]. The concentrations of cytokines and chemokines in culture supernatants were determined with a Cytometric Bead Array (CBA) (BD Biosciences, San Diego, CA, USA) according to the manufacturer's instructions.

3. Results

3.1. Differentiation into Monocyte-Macrophage–Lineage Cells of Human BM CD34⁺ Cells Cultured with a Combination of Cytokines

We first characterized the morphology and surface-antigen expression of human BM CD34⁺ cells cultured with the

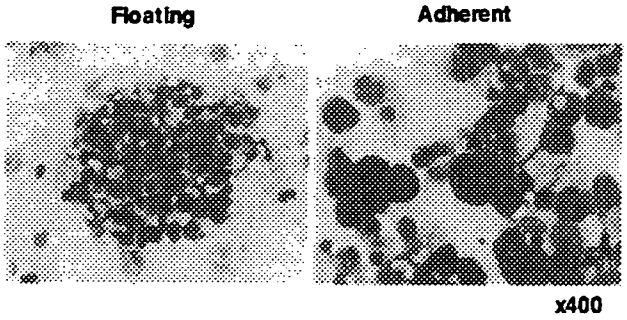

Figure 1. Morphology of monocyte-macrophage cells induced from CD34+ bone marrow (BM) cells in vitro. Human BM CD34+ cells were cultured for 5 weeks in the presence of a cytokine mixture, as described in "Materials and Methods." Floating and adherent cell fractions were subsequently collected separately and cytocentrifuged on a glass slide. Morphology was assessed after Giemsa staining. The experiments were repeated 3 times, and reproducible results were obtained. Representative data are shown (original magnification ×400).

combination of cytokines indicated in "Materials and Methods." During the second week of culture, microscopical observation revealed that a portion of the cells had started to adhere to the bottom of the culture dish. After 3 weeks of cultivation, the cells were clearly divided into floating and adherent fractions. When 1×10^5 CD34+ cells were cultured, approximately 7×10^6 adherent cells and 3×10^6 floating cells were obtained after 5 weeks of cultivation. At the end of the 5-week cultivation period, the floating and adherent fractions were collected separately, and their morphologies were assessed after May-Giemsa staining. As shown in Figure 1, the cells in the floating fraction were small and round and contained little cytoplasm. In contrast, the cells in the adherent fraction were large and contained abundant foamy cytoplasm with protrusions.

We also used flow cytometry to examine the cells for expression of monocyte-macrophage–lineage markers (Figure 2). Most floating cells expressed CD11b, CD31, CD33, and CD97, but no other mature-macrophage markers. The adherent cells, on the other hand, expressed markers of the myelocyte-monocyte lineage, such as CD13, CD14, CD36, CD54, CD64, CD85k, and CD105. It is noteworthy that the adherent cells expressed the mature-macrophage marker CD206, which was not expressed by the peripheral blood monocytes examined as a control (Figure 3).

3.2. Cytokine Secretion by Monocyte-Macrophage–Lineage Cells Induced from Human BM CD34+ Cells

Next, we assessed the cytokine-secreting ability of human BM CD34+ cells cultured with the cytokine combination. At the end of 5 weeks of cultivation, the floating and adherent fractions were collected separately, and cytokine secretion was assessed with the CBA system with and without LPS stimulation. Figure 4 shows that both the floating and adherent cell fractions spontaneously secreted IL-8 and IL-6 without LPS stimulation. After 24 hours of LPS stimulation, IL-6 secretion was enhanced in both fractions, but IL-8 secretion by adherent cells was decreased. TNF-α secretion, on the other hand, was induced in the 2 fractions only after LPS stimulation. It is noteworthy that LPS stimulation induced IL-10 secretion only in the adherent cell fraction and not in the floating cell fraction. Neither IL-1β nor IL-12 secretion was induced by LPS stimulation in either fraction.

We also used reverse transcriptase–polymerase chain reaction analysis to assess the effect of LPS stimulation on the expression levels of cytokine messenger RNA (mRNA). Consistent with the results of the CBA analysis, LPS stimulation enhanced the expression of TNF-α mRNA in both the adherent and floating cell fractions (Figure 5). IL-10 mRNA expression, however, was already detectable in both cell fractions in the unstimulated state, and LPS stimulation did not enhance expression. In addition, LPS stimulation reduced IL-10 mRNA expression in the floating cell fraction. It is interesting that although no secretion of IL-1β protein was detected by the CBA assay, LPS stimulation significantly increased IL-1β mRNA expression in both cell fractions.

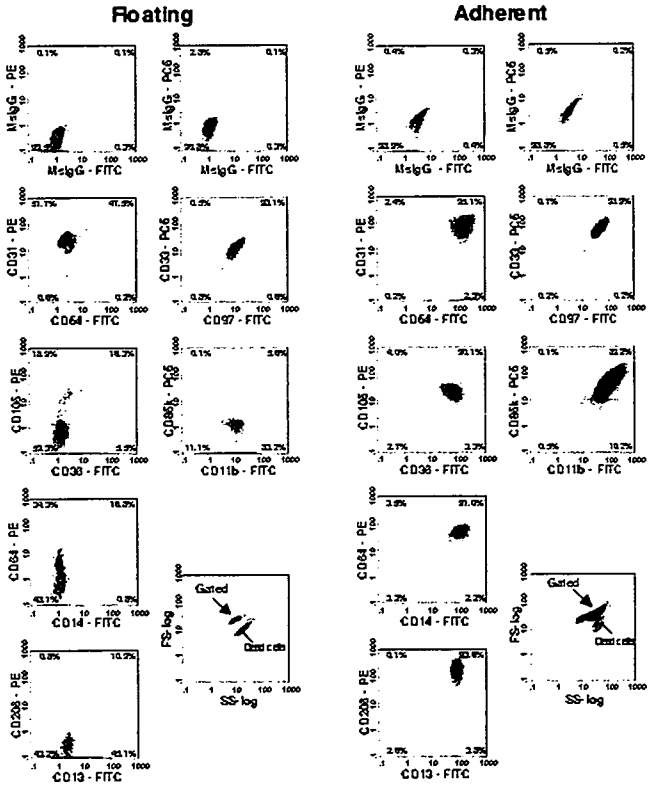

Figure 2. Immunophenotypic analysis of monocyte-macrophage cells induced from CD34+ bone marrow (BM) cells in vitro. Human BM CD34+ cells were cultured for 5 weeks (as in Figure 1). At the end of the culture period, the floating and adherent cell fractions were collected separately, stained with combinations of fluorescently labeled antibodies as indicated, and examined by flow cytometry. The experiments were repeated 3 times, and reproducible results were obtained. Representative histogram data are shown. MsIgG, mouse immunoglobulin G: PE, phycoerythrin; PC-5, PE-Cyanine 5; FITC, fluorescein isothiocyanate; FS, forward light scatter; SS, side light scatter.

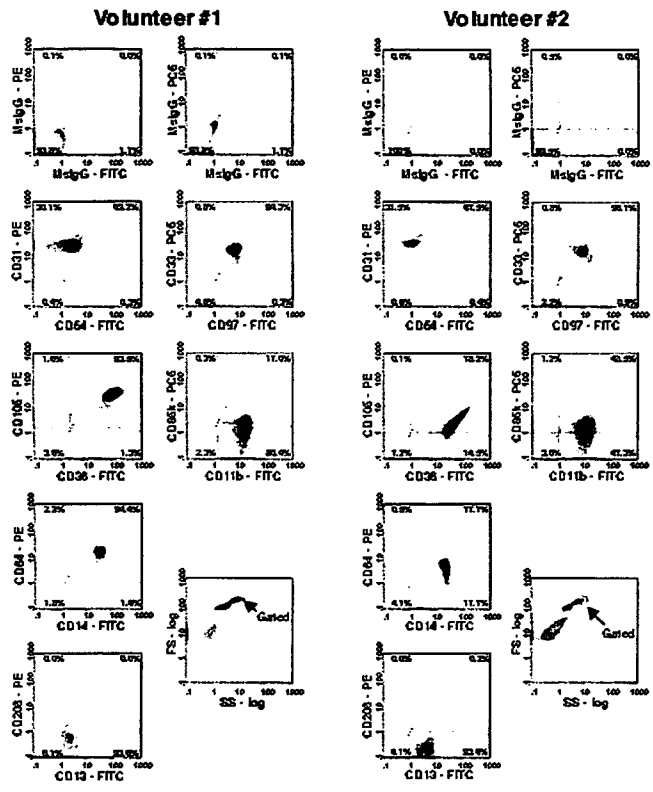

Figure 3. Immunophenotypic analysis of peripheral blood monocytes. Mononuclear cells were obtained from the peripheral blood of healthy volunteers via Ficoll-Paque centrifugation and stained with the indicated combinations of fluorescently labeled antibodies. Monocytes were gated, and the expression of each antigen was analyzed as in Figure 2.

3.3. Effect of G-CSF on TNF-α Secretion by Monocyte-Macrophage–Lineage Cells Induced from Human BM CD34⁺ Cells

As we reported previously, G-CSF directly affects peripheral blood monocytes and reduces LPS-induced TNF-α secretion in a time-dependent manner [20]. We therefore tested the effect of G-CSF on TNF-α secretion by monocyte-macrophage–lineage cells induced from human BM CD34⁺ cells. Because our testing of monocyte-macrophage–lineage cells that had been induced with cytokines and harvested after 5 weeks of cultivation showed that G-CSF did not affect LPS-induced TNF-α secretion (data not shown), we tested cells harvested at different time points. Our assessment of LPS-stimulated cytokine secretion by adherent cells (Figure 6) (but not floating cells; data not shown) collected after 3 weeks of cultivation revealed cytokine-secretion patterns different from those of cells collected after 5 weeks of cultivation. Figure 6 shows that cells cultured for 3 weeks spontaneously secreted low levels of IL-8, but not other cytokines. LPS stimulated the cells to secrete IL-6 and TNF-α and an increased level of IL-8. Pretreatment with G-CSF reduced LPS-induced TNF-α secretion in a time-dependent manner.

4. Discussion

This study has shown that monocyte-macrophage–lineage cells were efficiently induced from CD34⁺ BM cells in liquid culture in the presence of a cocktail of cytokines and that the monocyte-macrophage–lineage cells induced in vitro were capable of cytokine secretion upon stimulation with LPS. Several different subsets of monocyte-macrophage–lineage cells were induced during the course of culture.

For example, 2 distinct fractions, adherent cells and floating cells, were observed at the end of 5 weeks of culture. These 2 fractions were distinctive in both morphology and immunophenotype. Adherent cells were large, had a macrophage-like appearance, and expressed the mature-macrophage markers CD14, CD105, and CD206. In contrast, the floating cells were relatively small and contained little cytoplasm. Only some of them expressed mature-macrophage markers, whereas most

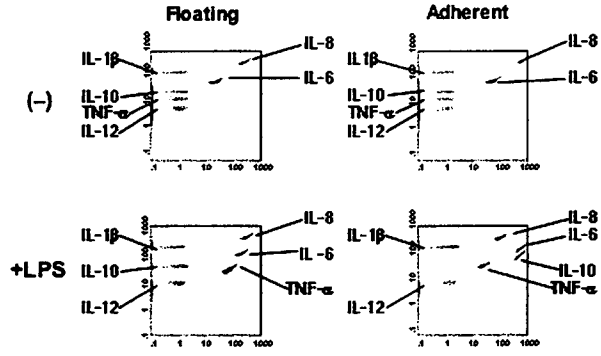

		Floating, ng/mL	Adherent, ng/mL
IL-8	(-)	9.24	26.13
	LPS	12.03	3.90
IL-1 β	(-)	0.07	0.07
	LPS	0.07	0.10
IL-6	(-)	0.87	2.03
	LPS	7.35	20.30
IL-10	(-)	0.02	0.02
	LPS	0.02	34.62
TNF-α	(-)	<0.00	<0.00
	LPS	2.55	0.87
IL12	(-)	<0.00	<0.00
	LPS	<0.00	<0.00

Figure 4. Cytometric Bead Array (CBA) analysis of lipopolysaccharide (LPS)-stimulated cytokine secretion by monocyte-macrophage cells induced from CD34⁺ bone marrow (BM) cells in vitro. Monocyte-macrophage–lineage cells were induced from human BM CD34⁺ cells by cultivation for 5 weeks, as described for Figure 1. At the end of the culture period, the floating and adherent cells were stimulated with and without LPS for 24 hours. Subsequent cytokine secretion was assessed with the CBA system. The histograms obtained (upper panels) and calculated concentrations of each cytokine (table at bottom; <0.00 indicates undetectable) are shown. The experiments were repeated 3 times, and reproducible results were obtained. Representative data are shown. IL-1β indicates interleukin 1β; TNF-α, tumor necrosis factor α.

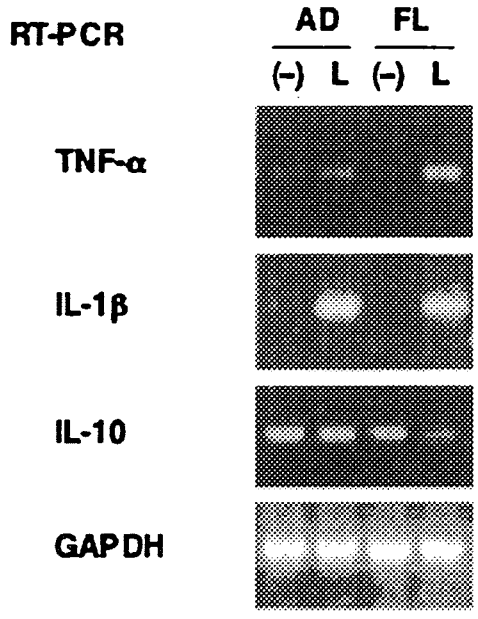

Figure 5. Reverse transcriptase–polymerase chain reaction (RT-PCR) analysis of lipopolysaccharide (LPS)-stimulated cytokine production by monocyte-macrophage cells induced from CD34+ bone marrow (BM) cells in vitro. Monocyte-macrophage–lineage cells were induced from human BM CD34+ cells as described for Figure 1, and then floating (FL) and adherent (AD) cell fractions were collected separately. After stimulation with (L) or without (–) LPS for 24 hours (as described for Figure 4), total RNA was extracted, and the indicated messenger RNA molecules were analyzed by the RT-PCR after complementary DNA synthesis. The experiments were repeated 3 times, and reproducible results were obtained. Representative data are shown. TNF-α indicates tumor necrosis factor α; IL-1β, interleukin 1β; GAPDH, glyceraldehyde-3-phosphate dehydrogenase.

cells expressed myelomonocytic antigens, including CD31, CD33, and CD97. It is interesting that these 2 fractions exhibited different cytokine-secretion abilities. Figure 4 shows that both fractions spontaneously secreted IL-8 and IL-6, and they both secreted TNF-α upon stimulation with LPS. Only the adherent cell fraction secreted IL-10 after LPS stimulation, however. These characteristics suggest that the adherent cell fraction represents mature macrophages, whereas the floating cell fraction may be related to immature monocytes. Evidence that further cultivation of the floating cell fraction induced an adherent cell fraction (data not shown) supports this idea.

It is noteworthy that both cell fractions contained more IL-1β mRNA after LPS stimulation but that no IL-1β secretion at the protein level was detected in either fraction. The data indicate that monocyte-macrophage–lineage cells induced in vitro are capable of producing IL-1β upon stimulation with LPS but that the stimulation is insufficient to induce secretion of IL-1β.

On the other hand, the adherent cells exhibited a profile of cytokine secretion after 3 weeks of cultivation that was distinct from that obtained after 5 weeks. At 3 weeks, the adherent cell fractions displayed almost the same immunophenotype as monocyte-macrophage–lineage cells cultured for 5 weeks; however, the cells spontaneously secreted only low levels of IL-8, and not other cytokines. Although the cells secreted IL-6 and TNF-α after LPS stimulation, they did not secrete IL-10. Thus, our data indicate that different culture conditions induce different monocyte-macrophage–lineage subsets or monocyte-macrophage–lineage cells with different degrees of maturity.

Several studies have shown the induction of monocyte-macrophage–lineage cells by in vitro culture of cells from different cell sources. For example, Akagawa reported that M-CSF–induced monocyte-derived macrophages (M-Mphi) and GM-CSF–induced Mphi (GM-Mphi) differ in morphology, cell surface antigen expression, and function, including Fcγ receptor–mediated phagocytosis, hydrogen peroxide production and sensitivity, catalase activity, susceptibilities to human immunodeficiency virus type 1 and *Mycobacterium tuberculosis*, and suppressor activity [21]. She therefore concluded that the characteristics of GM-Mphi resemble those of human alveolar macrophages. Servet-Delprat et al also

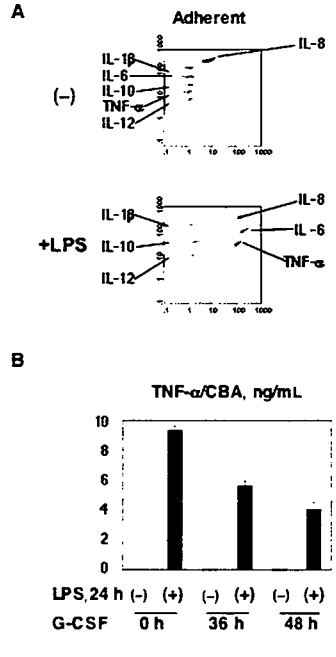

		Adherent, ng/mL
IL-8	(-)	0.58
	LPS	13.18
IL-1β	(-)	0.18
	LPS	0.22
IL-6	(-)	0.06
	LPS	16.7
IL-10	(-)	0.09
	LPS	0.17
TNF-α	(-)	0.03
	LPS	9.31
IL12	(-)	0.05
	LPS	0.09

Figure 6. Effect of granulocyte colony-stimulating factor (G-CSF) on lipopolysaccharide (LPS)-stimulated tumor necrosis factor α (TNF-α) secretion by monocyte-macrophage cells induced from CD34+ bone marrow (BM) cells in vitro. A, Monocyte-macrophage–lineage cells were induced from human BM CD34+ cells after 3 weeks of cultivation in the presence of the mixture of cytokines described in "Materials and Methods." At the end of the culture period, cells were stimulated with LPS for 24 hours. Subsequent cytokine secretion was assessed as in Figure 4. B, Induced monocyte-macrophage cells pretreated and not pretreated with G-CSF were stimulated with (+) and without (–) LPS for 24 hours, and subsequent cytokine secretion was assessed as in (A). The experiment was performed in triplicate, and the data are presented as the mean + SD. The experiments were repeated 3 times, and reproducible results were obtained. Representative data are shown. IL-1β indicates interleukin 1β.

reported that a variety of monocyte-macrophage–lineage cells, including macrophages, osteoclasts, dendritic cells, and microglia, can be induced from murine BM cells by ex vivo culture with different combinations of cytokines [22]. These reports further support our hypothesis that different culture conditions can induce different subsets of monocyte-macrophage–lineage cells.

In conclusion, the results of this study indicate that monocyte-macrophage–lineage cells induced from CD34⁺ BM cells in vitro can be used for functional assays, at least in terms of cytokine secretion. Further investigation is clearly necessary, however; the establishment of culture conditions that enable the induction of different subsets of monocyte-macrophage–lineage cells should provide an ideal experimental model for the analysis of monocyte-macrophage–lineage cell function.

Acknowledgments

This work was supported in part by Health and Labour Sciences Research Grants; a grant for Child Health and Development from the Ministry of Health, Labour and Welfare of Japan; and a grant from the Japan Health Sciences Foundation for Research on Health Sciences Focusing on Drug Innovation, JSPS. This work was supported by KAKENHI 17591131 and 18790751, the Budget for Nuclear Research of the Ministry of Education, Culture, Sports, Science and Technology, based on screening and counseling by the Atomic Energy Commission. This work was also supported by CREST, JST, and a grant from the Charitable Trust Japan Leukemia Research Fund. We thank S. Yamauchi for excellent secretarial work.

References

1. Gordon S. The macrophage. *Bioessays*. 1995;17:977-986.
2. Banchereau J, Steinman RM. Dendritic cells and the control of immunity. *Nature*. 1998;392:245-252.
3. Steinman RM, Turley S, Mellman I, Inaba K. The induction of tolerance by dendritic cells that have captured apoptotic cells. *J Exp Med*. 2000;191:411-416.
4. Teitelbaum SL. Bone resorption by osteoclasts. *Science*. 2000;289: 1504-1508.
5. Perry VH. A revised view of the central nervous system microenvironment and major histocompatibility complex class II antigen presentation. *J Neuroimmunol*. 1998;90:113-121.
6. Elkabes S, DiCicco-Bloom EM, Black IB. Brain microglia/ macrophages express neurotrophins that selectively regulate microglial proliferation and function. *J Neurosci*. 1996;16:2508-2521.
7. Noda M, Nakanishi H, Nabekura J, Akaike N. AMPA-kainate subtypes of glutamate receptor in rat cerebral microglia. *J Neurosci*. 2000;20:251-258.
8. Crofton RW, Diesselhoff-den Dulk MM, van Furth R. The origin, kinetics, and characteristics of the Kupffer cells in the normal steady state. *J Exp Med*. 1978;148:1-17.
9. Thomas ED, Ramberg RE, Sale GE, Sparkes RS, Golde DW. Direct evidence for a bone marrow origin of the alveolar macrophage in man. *Science*. 1976;192:1016-1018.
10. Kennedy DW, Abkowitz JL. Mature monocytic cells enter tissues and engraft. *Proc Natl Acad Sci USA*. 1998;95:14944-14949.
11. Takahashi K, Naito M, Takeya M. Development and heterogeneity of macrophages and their related cells through their differentiation pathways. *Pathol Int*. 1996;46:473-485.
12. Yamamoto T, Naito M, Moriyama H, et al. Repopulation of murine Kupffer cells after intravenous administration of liposome-encapsulated dichloromethylene diphosphonate. *Am J Pathol*. 1996;149: 1271-1286.
13. Wijffels JF, Hendrickx RJ, Steenbergen JJ, Eestermans IL, Beelen RH. Milky spots in the mouse omentum may play an important role in the origin of peritoneal macrophages. *Res Immunol*. 1992; 143:401-409.
14. Lawson LJ, Perry VH, Gordon S. Turnover of resident microglia in the normal adult mouse brain. *Neuroscience*. 1992;48:405-415.
15. Sawano A, Iwai S, Sakurai Y, et al. Flt-1, vascular endothelial growth factor receptor 1, is a novel cell surface marker for the lineage of monocyte-macrophages in humans. *Blood*. 2001;97:785-791.
16. Taghon T, Stolz F, De Smedt M, et al. HOX-A10 regulates hematopoietic lineage commitment: evidence for a monocyte-specific transcription factor. *Blood*. 2002;99:1197-1204.
17. Miyamoto T, Ohneda O, Arai F, et al. Bifurcation of osteoclasts and dendritic cells from common progenitors. *Blood*. 2001;98:2544-2554.
18. Xu MJ, Tsuji K, Ueda T, et al. Stimulation of mouse and human primitive hematopoiesis by murine embryonic aorta-gonad-mesonephros-derived stromal cell lines. *Blood*. 1998;92: 2032-2040.
19. Kiyokawa N, Kokai Y, Ishimoto K, Fujita H, Fujimoto J, Hata JI. Characterization of the common acute lymphoblastic leukaemia antigen (CD10) as an activation molecule on mature human B cells. *Clin Exp Immunol*. 1990;79:322-327.
20. Saito M, Kiyokawa N, Taguchi T, et al. Granulocyte colony-stimulating factor directly affects human monocytes and modulates cytokine secretion. *Exp Hematol*. 2002;30:1115-1123.
21. Akagawa KS. Functional heterogeneity of colony-stimulating factor-induced human monocyte-derived macrophages. *Int J Hematol*. 2002;76:27-34.
22. Servet-Delprat C, Arnaud S, Jurdic P, et al. Flt3⁺ macrophage precursors commit sequentially to osteoclasts, dendritic cells and microglia. *BMC Immunol*. 2002;3:15.

ELSEVIER

Experimental Hematology

Experimental Hematology 35 (2007) 1398–1407

Interleukin-7 contributes to human pro–B-cell development in a mouse stromal cell–dependent culture system

Tomoko Taguchi[a,b], Hisami Takenouchi[a], Yusuke Shiozawa[a], Jun Matsui[a], Noriko Kitamura[a], Yoshitaka Miyagawa[a], Yoko U. Katagiri[a], Takao Takahashi[b], Hajime Okita[a], Junichiro Fujimoto[a], and Nobutaka Kiyokawa[a]

[a]*Department of Developmental Biology, National Research Institute for Child Health and Development, Setagaya-ku, Tokyo, Japan;* [b]*Department of Pediatrics, Keio University, School of Medicine, Shinjuku-ku, Tokyo, Japan*

(Received 20 March 2007; revised 10 May 2007; accepted 31 May 2007)

Objective. **The role of interleukin (IL)-7 in human B lymphopoiesis is still controversial. We used an in vitro culture system to verify involvement of IL-7 in development of human pro-B cells from hematopoietic stem cells.**

Materials and Methods. **Human CD34$^+$ bone marrow cells were cultured for 4 weeks on MS-5 mouse stromal cells to induce pro-B cells. Expression of IL-7 receptor α or other B-cell differentiation marker genes on cultured human CD34$^+$bone marrow cells was investigated by reverse transcription polymerase chain reaction (RT-PCR). Colony assay of human CD34$^+$ bone marrow cells was also performed to determine the effect of IL-7 on colony-forming ability. Neutralizing antibody or reagent that eliminates the effect of IL-7 was added to the culture system, and the number of pro-B cells induced was estimated by flow cytometry.**

Results. **RT-PCR analysis revealed mRNA expression of IL-7 receptor α as well as B-cell differentiation marker genes in not only CD19$^+$ pro-B cells but also CD19$^-$ CD33$^-$ cells induced from CD34$^+$ bone marrow cells after cultivation for 4 weeks on MS-5 cells. Addition of anti-mouse IL-7 antibody, anti-human IL-7 receptor α antibody, or JAK3 kinase inhibitor reduced the number of pro-B cells induced, demonstrating that elimination of IL-7 reduces pro–B-cell development. Addition of anti-mouse IL-7 antibody emphasized the colony-forming ability of burst-forming unit erythroid cells.**

Conclusions. **IL-7 produced by MS-5 cells is required for human pro–B-cell development from CD34$^+$bone marrow cells in our culture system, and IL-7 appears to play a certain role in early human B lymphopoiesis.** © **2007 ISEH - Society for Hematology and Stem Cells. Published by Elsevier Inc.**

Interleukin (IL)-7 is a cytokine that was first cloned from a murine bone marrow (BM) stromal cell line and is involved in the regulation of lymphopoiesis [1]. Several studies have shown that IL-7 is crucial to proliferation and development of murine B cells. For example, injection of mice with recombinant IL-7 has been shown to greatly increase the number of B cells [2], whereas injection of anti–IL-7 antibodies severely represses B-cell development [3,4]. Study of the effect of IL-7 on fractionated B-lineage cells from normal mouse BM in a stromal-cell–dependent culture system revealed that IL-7 is required for effective differentiation of pro-B cells into pre-B cells [5]. IL-7 is sufficient to induce differentiation of murine common lymphoid progenitors into pro-B cells in cultures under stromal-cell–free conditions [6].

The requirement for IL-7 in B-lymphocyte development in mice was further demonstrated by experiments in which components of the IL-7 signal transduction pathways were deleted by gene targeting [7–10]. Results showed that B-cell development is severely arrested at the common lymphoid progenitor stage in the BM of adult IL-7 receptor (R) α and common γ-chain–deficient mice, leading to a striking paucity of peripheral B cells.

In contrast to murine B-cell development, however, human B-cell development does not appear to require IL-7

Offprint requests to: Nobutaka Kiyokawa, M.D., Ph.D., Department of Developmental Biology, National Research Institute for Child Health and Development, 2-10-1, Okura, Setagaya-ku, Tokyo 154-8535, Japan; E-mail: nkiyokawa@nch.go.jp

0301-472X/07 $–see front matter.
doi: 10.1016/j.exphem.2007.05.019

[11]. Unlike the mouse common γ knockouts, patients with human X-linked severe combined immunodeficiency, who lack a functional common γ chain, produce normal numbers of B cells [12]. Immunodeficiency patients with autosomal recessive mutations in either IL-7Rα chain or JAK3 tyrosine kinase, a downstream signaling molecule of IL-7R, also have normal numbers of peripheral B cells [13–15]. All of this evidence indicates that IL-7 is not always required for B-cell development in humans.

Nevertheless, some studies found that IL-7 affects human B-cell development in some way. For example, it was found that IL-7 transduces signals that lead to specific changes in gene expression during human B-cell development. IL-7 stimulation induces a specific increase in CD19 on the surface of human pro-B cells and decrease in RAG-1, RAG-2, and TdT messenger RNA levels [16]. Proliferation of $CD19^+CD34^+$ pro-B cells on human BM stromal cells is enhanced by inclusion of exogenous IL-7 in the culture [17]. Therefore, if not essential, IL-7 may play an integral role in some aspects of human B-cell development.

In an attempt to clarify the effect of IL-7 on human B-cell development, we used an in vitro culture system in which human hematopoietic stem cells are cocultured with murine BM stromal cells that induce pro–B-cell differentiation. In this article, we report finding that IL-7 is essential for the differentiation of human $CD34^+$ BM cells into pro-B cells in our culture system, and we discuss the possible role of IL-7 in early human B-cell development.

Materials and methods

Reagents

Monoclonal antibodies used were phycoerythrin (PE)-conjugated anti-CD33, from Becton Dickinson Biosciences (San Diego, CA, USA), and PE-cyanine (PC)-5–conjugated anti-CD19, from Beckman/Coulter Inc. (Westbrook, MA, USA). Goat polyclonal anti-mouse IL-7 antibody (Ab) and goat anti-human IL-7Rα Ab were obtained from R&D Systems (Abingdon, UK) and used in the cultures at concentrations of 1 to 5 μg/mL, as indicated. Recombinant human IL-2, -4, -7, -9, and -11 were obtained from PeproTech EC Ltd. (London, UK) and recombinant human IL-15, -21, and both human and mouse thymic stromal lymphopoietin (TSLP) were obtained from R&D Systems.

4-[(3′-Bromo-4′-hydroxyphenyl) amino]-6,7-dimethoxyquinazoline, a potent specific inhibitor of JAK3 kinase (IC_{50} = 5.6 μM) was obtained from Calbiochem-Novabiochem Co. (San Diego, CA, USA) and used in the cultures at a concentration of 5 μM. The specificity of this chemical compound as a JAK3 kinase inhibitor has been examined by Goodman et al. [18] and Sudbeck et al. [19]. They demonstrated that this compound exhibited detectable inhibitory activity only against recombinant JAK3, but not JAK1 or JAK2, in immune complex kinase assays and also inhibited IL-2–induced JAK3-dependent signal transducers and activators of transcription (STAT) activation, but not inhibited IL-3–induced JAK1/JAK2-dependent STAT activation in 32Dc11-IL2R cells. Unless otherwise indicated, all chemical reagents were obtained from Wako Pure Chemical Industries, Ltd. (Osaka, Japan).

Cells, cultures, and colony assay

Human BM $CD34^+$ cells used were purchased from Cambrex Bio Science Walkersville, Inc. (Walkersville, MD, USA). BM cells were isolated from human tissue after obtaining informed consent. A cloned murine BM stromal cell line, MS-5, was kindly provided by Dr. A. Manabe (St. Luke's International Hospital, Tokyo, Japan) and Dr. K. Mori (Nigata University, Nigata, Japan), and maintained in RPMI-1640 medium (Sigma-Aldrich Fine Chemical Co., St. Louis, MO, USA) supplemented with 10% (v/v) fetal calf serum (Sigma-Aldrich) at 37°C under a humidified 5% CO_2 atmosphere.

To induce pro-B cells, MS-5 cells were plated at a concentration of 1×10^5 cells in 12-well tissue plate (Asahi Techno Glass Co., Chiba, Japan) 1 day prior to seeding human BM $CD34^+$ cells. $CD34^+$ cells were plated 4×10^4 cells/well/2 mL onto the MS-5 cells in RPMI-1640 supplemented with 10% fetal calf serum and

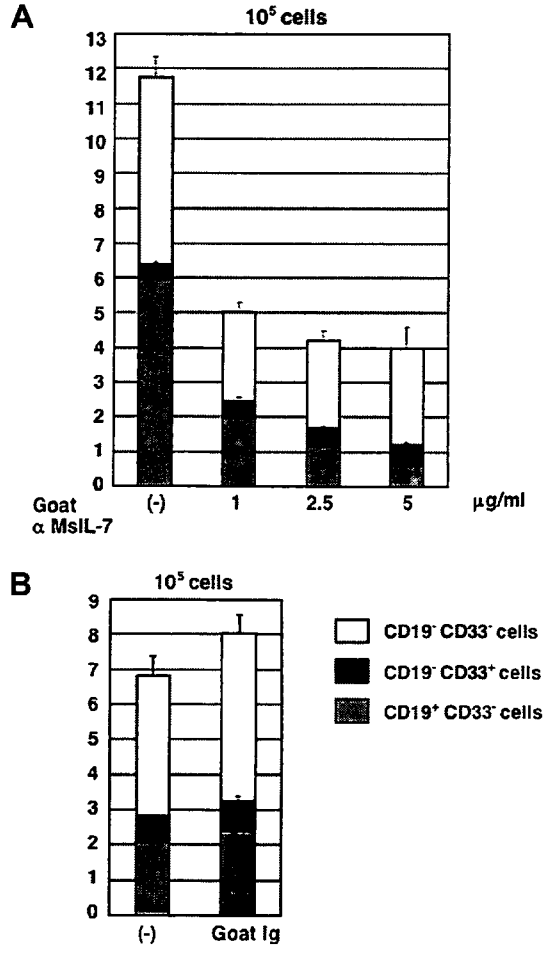

Figure 1. Effect of anti-mouse interleukin (IL)-7 antibody on human pro–B-cell development. (**A**) Human bone marrow $CD34^+$ cells were cultured on MS-5 cells for 4 weeks in the presence or absence {(–)} of different concentrations of goat polyclonal anti-mouse IL-7 antibody. The subsequent $CD19^+CD33^-$ cell number (lower light gray column), $CD19^-CD33^+$ cell number (middle dark gray column), and $CD33^-CD19^-$ cell number (upper white column) of cultured $CD34^+$ cells were calculated by flow cytometry. (**B**) Human bone marrow $CD34^+$ cells were cultured on MS-5 cells for 4 weeks in the presence or absence of goat immunoglobulin (goat Ig) as a negative control.

various combinations of cytokines or other reagents, as indicated in Figures 1,3,5,6,8. After cultivation for the periods indicated, the cells were harvested with 0.25% trypsin plus 0.02% ethylenediamine tetraacetic acid (IBL Co. Ltd., Gunma, Japan), the number of cells per well was counted, and cells were analyzed by flow cytometry.

For the colony assay, $CD34^+$ BM cells were cultured for 1 week on MS-5 cells in the presence or absence of goat anti-IL-7 Ab and the floating cell fraction was first collected with culture medium. The remaining adherent cell fraction with MS-5 cells were treated with trypsin, harvested, and plated in 6-well tissue culture plate (Asahi Techno Glass). After removing MS-5 cells by letting them attach to the bottom of the plate by 15-minute incubation, subsequent suspension cells were collected as adherent cell fraction. After counting the cell number by flow cytometry using Flow-Count (Beckman/Coulter), cells from each fraction were passaged into methylcellulose cultures containing the cocktail of cytokines (MethocultTM GF+H4435; Stem Cell Technologies Inc, Northampton, UK). Morphology and number of colonies comprising more than 50 cells was scored at 14 days. All experiments were performed in triplicate and the mean + SD of the values were shown in Figures 1,3,5,6,8.

Immunofluorescence study

Cells were stained with fluorescence-labeled monoclonal antibodies and analyzed by flow cytometry (EPICS-XL, Beckman/Coulter) as described previously [20]. Two-color immunofluorescence study was performed with a combination of PE and PC-5. Experiments were performed in triplicate, and the mean + SD of the cell counts were indicated in the Figures 1,3,5,6,8.

For cell sorting, human BM $CD34^+$ cells cocultured with MS-5 cells for 4 weeks were harvested and stained with PE-conjugated anti-CD33 monoclonal Ab and PC-5–conjugated anti-CD19 monoclonal Ab. $CD33^-CD19^-$, $CD33^+$ and $CD19^+$ cells were sorted in an EPICS-ALTRA cell sorter (Beckman/Coulter). Total RNA was extracted and used for reverse transcription polymerase chain reaction (RT-PCR).

RT-PCR

Total RNA was extracted from cultured cells, and cDNA was generated with an RNeasy Mini Kit (Qiagen, Valencia, CA, USA) and a FirstStrand cDNA Synthesis Kit (Pharmacia Biotech, Uppsala, Sweden). cDNA synthesized from 150 ng total RNA was used as a template for one amplification. The sets of primers used in this study were listed in Table 1.

PCR was repeated for 30 to 35 cycles of heating at 94°C for 60 seconds, annealing at 60°C for 30 seconds, and elongation at 72°C for 2 minutes; the products were then separated on a 1.5% agarose gel.

Results

MS-5 cells secrete IL-7

Murine stromal cell line MS-5 has been reported to possess the ability to support the differentiation of B-lineage cells and myeloid cells from human cord blood $CD34^+$ cells [21–25]. Consistent with previous observations, the human BM $CD34^+$ cells in our study generated $CD19^+CD33^-$ B cells and $CD19^-CD33^+$ myeloid cells after 4 weeks of

Table 1. List of primers used in this study

Name of gene	Primer sequence	Product size (bp)
Murine IL-7		
Forward	5′-TAAATCGTGCTGCTCGCAAGT-3′	
Reverse	5′-AGCAGTCAGCTGCATTTCTGTG-3′	392
Human IL-7R α		
Forward	5′-GTCACTCCAGAAAGCTTTGG-3′	
Reverse	5′- AGGAACTCTAGACTTCCCTTT-3′	
Human CD19		
Forward	5′-GTTCCGGTGGAATGTTTCGG-3′	386
Reverse	5′-AGATGAAGAATGCCCACAAGG-3′	576
Human TdT		
Forward	5′-ACACGAATGCAGAAAGCAGGA-3′	
Reverse	5′-AGGCAACCTGAGCTTTTCAAA-3′	315
Human PAX5		
Forward	5′-CCATCAAGTCCTGAAAAATC-3′	
Reverse	5′-CCCAAAGTGGTGGAAAAAAT-3′	319
Human Igα		
Forward	5′-TAGTCGACATGCCTGGGGGTCCAGGAGTCCTC-3′	
Reverse	5′-GATGTCCAGCTGGAGAAGCCGTGA-3′	681
Human GAPDH		598
Forward	5′-CCACCCATGGCAAATTCCATGGCA-3′	
Reverse	5′-TCTAGACGGCAGGTCAGGTCCACC-3′	
Murine actin		
Forward	5′-TGACGGGGTCACCCACACTGTGCCCATCTA-3′	
Reverse	5′-CTAGAAGCATTTGCGGTGGACGATGGAGGG-3′	661

GAPDH = glyceraldehyde phosphate dehydrogenase; IL = interleukin.

cocultivation with MS-5 cells (Fig. 1). Immunocytological analysis showed that the $CD19^+$ B cells in our culture system were surrogate light $chain^+$ μ^- pro-B cells [25]. Consistent with these observations, the human BM $CD34^+$ cells in our study generated $CD19^+$ B cells and $CD33^+$ myeloid cells after 4 weeks of cocultivation with MS-5 cells (Fig. 1). The detailed characterization of our culture system has been reported previously [25]. Starting with 4×10^4 $CD34^+$ cells, that containing <8% of $CD19^+CD34^+$, 0.4 to 1.3×10^6 mononuclear cells, 30.1% to 68.2% of which were $CD19^+CD34^-$ cells, were obtained (data not shown). Immunocytological analysis showed that most of these $CD19^+$ B cells expressed cytoplasmic-CD179a, a component of surrogate light chain known to be most specific molecular marker of precursor-B cells, whereas only a few percent of the $CD19^+$ cells were positive for surface and/or cytoplasmic-μ^- heavy chain. Considering the additional observations that CD10, CD24, and CD43 were expressed but CD20 were not in the $CD19^+$ cells, we concluded that most of the $CD19^+$ B cells obtained in our culture system were pro-B cells [25].

We investigated the expression of IL-7 by the MS-5 cells and IL-7Rα by cultured $CD34^+$ BM cells. RT-PCR analysis showed expression of murine IL-7 by MS-5 cells (Fig. 2A). In addition, expression of human IL-7Rα mRNA by the cultured human BM $CD34^+$ cells was observed (Fig. 2B).

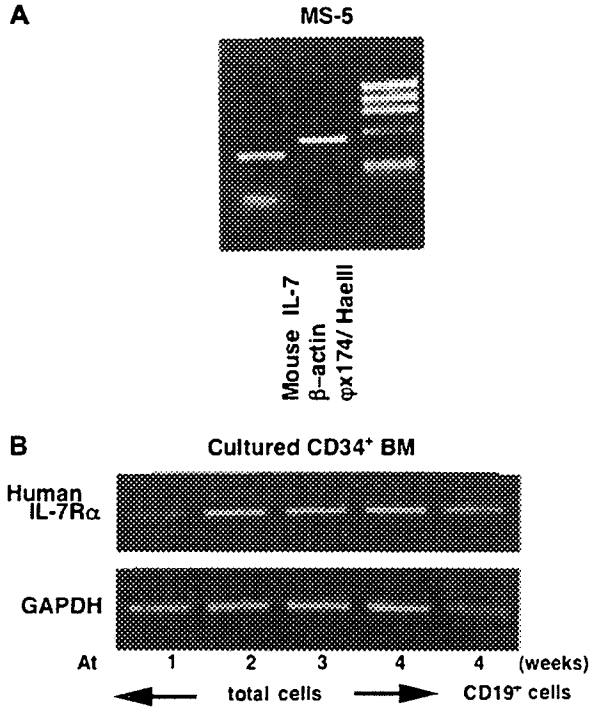

Figure 2. Expression of interleukin (IL)-7 by murine stromal MS-5 cells and of IL-7 receptor by cultured human bone marrow $CD34^+$ cells. (**A**) Expression of IL-7 by MS-5 cells was investigated by reverse transcription polymerase chain reaction (RT-PCR). Expression of mouse β-actin was also investigated as an internal control. The $\phi\chi174$/*Hae*III molecular weight marker is shown on the right side. (**B**) Human bone marrow $CD34^+$ cells cultured on MS-5 cells for 1, 2, 3, and 4 weeks. At the end of each culture period, cultured human bone marrow cells was collected by gentry pipetting, and the expression of IL-7 receptor (R) α was investigated by RT-PCR. $CD19^+$ cells were sorted from 4-week cultured human bone marrow $CD34^+$ cells and similarly examined. Expression of human glyceraldehyde phosphate dehydrogenase was investigated as an internal control.

Elimination of IL-7 reduced pro–B-cell development

Because murine IL-7 is known to react with human IL-7R [26], the IL-7 secreted by MS-5 cells possibly affects cultured $CD34^+$ BM cells. We therefore investigated the effect of anti-mouse IL-7 antibodies, which neutralizes the effect of IL-7 on cultured $CD34^+$ BM cells. As shown in Figure 1, when anti-mouse IL-7 Ab was added, the $CD19^+CD33^-$ B-cell development was significantly reduced. In contrast, when goat immunoglobulin (Ig) G was similarly added, as a control experiment for Figure 1A, the $CD19^+CD33^-$ B-cell development was not reduced (Fig. 1B), indicating that the effect of anti-mouse IL-7 Ab is specific. The inhibitory effect of anti-mouse IL-7 Ab on pro–B-cell differentiation was found to be dose-dependent and time-dependent (Figs. 1 and 3). It is noteworthy that no significant change in $CD19^-CD33^+$ myeloid cell development was observed, whereas the subsequent cell number of $CD19^-CD33^-$ was also suppressed by addition of anti-mouse IL-7 Ab (Fig. 1).

Because we observed the inhibitory effect of anti-mouse IL-7 Ab on $CD19^-CD33^-$ cell fraction, we next investigated the expression of B-lineage marker genes to evaluate more detail characterization of these cells. As shown in Figure 4A, in addition to $CD19^+CD33^-$ pro–B cell, $CD19^-CD33^-$ cells but not $CD19^-CD33^+$cells also expressed IL-7Rα, after cultivation for 4 weeks. Expression of TdT was also detected in $CD19^-CD33^-$ cells. Although 30 cycles amplification failed in detection of PAX5 and Igα genes, 35 cycles amplification revealed the expression of these genes in $CD19^-CD33^-$ cells (Fig. 4B).

Effect of elimination of IL-7 on colony formation of $CD34^+$ BM cells

We also examined the effect of IL-7 elimination on colony formation ability of $CD34^+$ BM cells. The $CD34^+$ cells were cultured on MS-5 cells with and without anti-mouse IL-7 Ab for 1 week and examined by colony formation assay. As we reported previously [25], cultured $CD34^+$ cells on MS-5 cells can be classified into two subpopulations, namely, floating and adherent cell fraction. Interestingly, treatment with anti-mouse IL-7 Ab distinctively affected each cell fraction and the number of adherent cells was slightly decreased, whereas the floating cells were not reduced (Fig. 5A). Moreover, after treatment with anti-mouse IL-7 Ab, granulocyte-erythrocyte-macrophage-megakaryocyte (GEMM) colony formation from floating cells was slightly reduced and burst-forming unit erythroid (BFU-E) colony formation

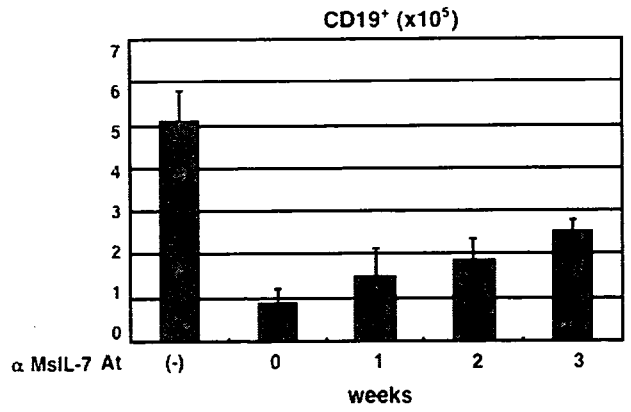

Figure 3. Time-dependency of anti-mouse interleukin (IL)-7 antibody–mediated inhibition of pro–B-cell development. Human bone marrow $CD34^+$ cells were cultured on MS-5 cells for 4 weeks. Goat polyclonal anti-mouse IL-7 antibody (2.5 μg/mL) was added at the start of culture (0), and after 1, 2, and 3 weeks of culture, and the number of $CD19^+$ cells was estimated by flow cytometry.

from adherent cells was significantly increased (Fig. 5B). Especially, subsequent BFU-E colony formation from total cells was also increased by anti-mouse IL-7 Ab treatment.

Effect of cytokines on anti–IL-7 Ab-mediated reduction in B-cell development

Since the reduction in $CD19^+$ B-cell development induced by anti-mouse IL-7 Ab was reversed by addition of recombinant human IL-7 to the coculture of $CD34^+$ BM cells and MS-5 cells (Fig. 6A), the effect of anti-mouse IL-7 Ab was concluded to be IL-7–specific. However, when we investigated the effect of exogenous recombinant human IL-7 alone, no significant increase in $CD19^+$ B-cell development was observed (Fig. 6A). Also, the proportion of different lineages cells was not affected by exogenous recombinant human IL-7 (data not shown). It is noteworthy that although exogenous recombinant human IL-7 did not change the number of pro-B cells, it increased the intensity of CD19 expression on $CD34^+$ BM cells (Fig. 7), while further differentiation of pro-B to pre-B cell was not observed (data not shown).

Next, we investigated the effect of exogenous recombinant human IL-2, IL-4, IL-9, IL-11, IL-15, and IL-21, which mediates signal transduction via common γ chain on the reduction in pro–B-cell development induced by anti-mouse IL-7 Ab, and no significant recovery in pro–B-cell development was observed (Fig. 6B). TSLP has been reported to mediate signal transduction via IL-7R and TSLPR heterodimer and have overlapping function with IL-7 [27,28]. Thus, we also investigated the effect of exogenous recombinant murine and human TSLP on reduction in pro–B-cell development induced by anti-mouse IL-7 Ab, whereas no significant recovery in pro–B-cell development was observed (Fig. 6C).

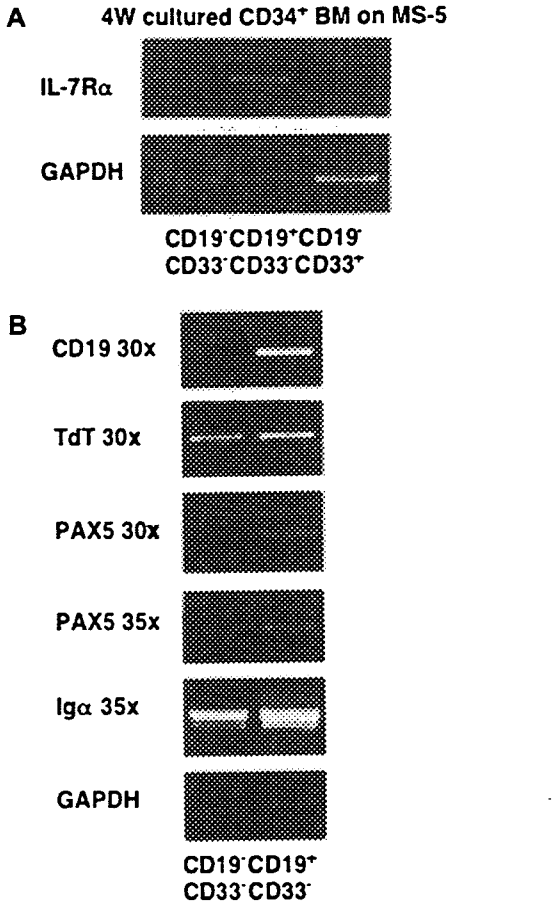

Figure 4. Expression of B-cell differentiation marker mRNAs by cultured human bone marrow $CD34^+$ cells. (**A**) Human bone marrow $CD34^+$ cells cultured on MS-5 cells for 4 weeks, $CD33^-CD19^-$, $CD33^+CD19^-$, and $CD33^-CD19^+$ cells were sorted, and expression of IL-7Rα was investigated by reverse transcription polymerase chain reaction with 30 cycles amplification. Expression of human glyceraldehyde phosphate dehydrogenase (GAPDH) was also investigated as an internal control. (**B**) $CD33^-CD19^-$ and $CD33^-CD19^+$ cells were sorted from 4-week cultured human bone marrow $CD34^+$ cells and expression of B-cell–differentiation marker genes as indicated were similarly examined as in (**A**) with either 30 or 35 cycles amplification. Expression of human GAPDH was investigated as an internal control.

Inhibition of IL-7 signaling reduced pro–B-cell development

Next, we investigated whether anti-human IL-7Rα Ab inhibits pro–B-cell development. As shown in Figure 8, addition of human IL-7Rα Ab that block the effect of IL-7 reduced the number of pro–B-cell development. Because IL-7R signaling transduces to JAK3, we investigated the effect of a JAK3 kinase inhibitor. As shown in Figure 8, the JAK3 kinase inhibitor significantly reduced pro–B-cell development.

Discussion

In this article, we demonstrated that IL-7 plays a certain role in development of human pro-B cells from